

ARTICLE

Microclimatic Zonation and Climatic Variability of Sikkim Himalaya

Pramod Kumar^{1,2*}, Kuldeep Dutta¹, Rakesh Kumar Ranjan¹, Nishchal Wanjari¹, Anil Kumar Misra¹

¹ Department of Geology, Sikkim University, Tadong, Gangtok, Sikkim, 737102, India

² Institute of Environment and Sustainable Development, Banaras Hindu University, Varanasi, UP, 221005, India

ABSTRACT

The Köppen classification of climate integrates precipitation and temperature information with natural vegetation patterns to create a precise representation of any particular region's climate. This integration depends on the empirical relationship of climate and vegetation, which indicates that distinct locations in the same class have similar vegetation attributes. Köppen climatic classification factors are explained and Sikkim's climate characteristics are regionalized based on it. The method for making representations of air temperatures and precipitation has been described, and an illustration of Sikkim's climatic zones with variability is generated as a result of these changes. The geographic pattern of climatic types and subtypes in Sikkim has been briefly addressed using an available high-resolution gridded dataset (ERA5-Land). This is described that the constraints of microclimatic zonation emanate from the empirical prerequisite of climate classifications, as well as the nature of data selection and the methodologies employed for climate variability analysis and classification. Based on the Köppen classification for the long term (1980–2021), the Sikkim Himalaya contains three primary climatic classes, particularly ETc (cold, tundra, and cool summer), Cfc (moderately warm, humid, and cool summer), and Cfb (moderately warm, humid, and warm summer). Climate variability on the basis of temperature and precipitation change with respect to 1980–2021 over the entire Sikkim Himalaya concludes that the climatic pattern of the Sikkim has been changed from cold-dry to warm-wet. The alteration in the corresponding climatic pattern is further supported by changes in LULC and NDVI. The results suggest that the precipitation change in the past two decades (1980–2000) is negative, while a significant positive change has been noticed in the recent two decades (2001–2021). Subsequently, the number of extremely wet days decreases in the entire ETc and Cfc climate zones. Regardless, the southern part of the Cfb climatic zone has experienced an increase in extremely wet days. This study's findings will significantly contribute to the development of future policies and initiatives by providing insights crucial for achieving sustainable development, environmental protection, and climate change adaptation.

Keywords: Climate variability; Köppen classification; Himalaya; ERA5-Land; Climate change impacts; Extremes

*CORRESPONDING AUTHOR:

Pramod Kumar, Department of Geology, Sikkim University, Tadong, Gangtok, Sikkim, 737102, India; Institute of Environment and Sustainable Development, Banaras Hindu University, Varanasi, UP, 221005, India; Email: promnagar1@gmail.com

ARTICLE INFO

Received: 23 May 2024 | Revised: 24 June 2024 | Accepted: 19 July 2024 | Published Online: 25 July 2024

DOI: <https://doi.org/10.30564/jasr.v7i3.6684>

CITATION

Kumar, P., Dutta, K., Ranjan, R.K., et al., 2024. Microclimatic Zonation and Climatic Variability of Sikkim Himalaya. Journal of Atmospheric Science Research. 7(3): 80–110. DOI: <https://doi.org/10.30564/jasr.v7i3.6684>

COPYRIGHT

Copyright © 2024 by the author(s). Published by Bilingual Publishing Group. This is an open access article under the Creative Commons Attribution-NonCommercial 4.0 International (CC BY-NC 4.0) License (<https://creativecommons.org/licenses/by-nc/4.0/>).

1. Introduction

Climate is the collection of averaged typical atmospheric variables that define a particular region and have a significant impact on ecosystems^[1]. The climate affects Human endeavors, especially agricultural and livestock establishment^[2,3]. The particular effects on crops and livestock are different by accessibility, depending on the regional environment, terrain, and farming/ranching strategies. Several economically developing nations (like India, and Pakistan, along with other Asian countries) centered substantially on the crops and livestock, rendering them particularly exposed to climate-related challenges^[4]. As a result, understanding the microclimate beforehand is of the utmost importance for agricultural development. Therefore, a prior understanding of the regionalized climate is essential for agricultural development^[5]. Climate classification is a strategy for characterizing climatic categories as well as spatiotemporal variability in the climate system^[6,7]. Besides, Holdridge (1967), Flohn (1950), Camargo (1991), Thornthwaite (1948), and Köppen and Geiger (1928) there are numerous other climatic classifications^[8]. Though, one of the most frequently used approaches to classify climates is the Köppen classification. Considering, that since natural vegetation provides an accurate representation of the climate over a particular area, the Köppen algorithm fundamentally integrates precipitation and temperature with the pattern of natural vegetation^[7]. Recent studies have considerably improved the Köppen-Geiger climate classification maps at a 1-kilometer resolution over the entire globe^[9–11]. The time period covered by these maps has also been extended, with data spanning from 1901 to 2020 and future projections up to 2099, offering precise information on climate patterns globally using multiple climate models^[9,11]. The Köppen classification has been employed in various fields of study such as agrometeorology, geography, and climatology in some European nations, China, Brazil, India and globally^[5,11–17]. In the context of the current climate crisis, this is one of the most concerning areas of research for the scientific community. Frequently extreme events (such

as torrential downpours, floods, and droughts) are an imminent risk to agriculture, ecological health, and socioeconomic well-being in the broader picture of global and regional changing climates^[17,18]. Climate change is also largely driven by variations in dryness and wetness. Changes in dryness and wetness have a significant effect on climate change; this is easily quantified, particularly using the Köppen climate classification system. For example, extreme fluctuations over dry and wet circumstances may have negative consequences for entire local and micro-regions^[19]. Consequently, a quantitative analysis of the development of local dry/wet patterns is essential to safeguard regional watersheds in considering climate change^[17].

The Himalaya is one of the important water resources for India as well as neighboring countries. Climate variability over mountainous regions is becoming more evident as global temperatures rise at a faster rate. The Köppen classification system has also been used to investigate the changing pattern of climatic characteristics for the mountainous region^[5,13–17]. Regional changes are occurring as the Köppen climatic region changes with latitude and altitude^[11]. Besides the effect of rising temperatures is not uniformly distributed. Some regions and months, especially the high mountain region, have experienced a much warmer temperature than the global mean^[11,17]. Therefore, the microclimate zonation provides an overview for analyzing a range of environmental and socioeconomic events and information as well as aids in our understanding of the type and subtype of climate. Furthermore, regional vegetation productivity is more adversely affected by the higher frequency and severity of extreme weather events than by long-term climate change. As an alternative, the use of vegetation activities as a proxy for changes in climate extremes became frequent^[20]. The application of the daily normalized difference vegetation index (NDVI) reveals the understanding of how vegetation responds to short-term climatic events^[21]. Moreover, the analysis of land use and land cover (LULC) and NDVI are useful in evaluating changes in regional geo-meteorology, particu-

larly in mountainous regions. The spatial-temporal change in LULC over some parts of the Himalayan regions has been studied to understand the geospatial variation and its connection with human-induced climate change^[22,23]. The Indian Himalayan Region (IHR) has experienced significant increases in urban areas, agricultural land, and built-up areas, meanwhile decreasing forest cover and water bodies^[22–25]. These variations are triggered by economic pressures, climate variability, and population growth^[23,26]. Furthermore, changes in LULC have an impact on Land Surface Temperature (LST) patterns, with shifts from low to medium and high LST categories resulting from LULC class conversions, such as agricultural land to horticulture and built-up areas in Indian Himalayan states^[27]. Additionally, there are many studies reported in order to understand the relationship involving various aspects (i.e., glacier, hydrology, aerosols, agriculture, and geography) of LULC and its spatial-temporal evolution of Sikkim Himalaya^[28–32]. However, a deeper understanding of the regional spatial-temporal effects of climatic variability, LULC, NDVI, and microclimatic zonation in the Sikkim Himalaya is still needed.

To establish an extensive understanding of regional climate zone shifts and variability, this work starts with an investigation into climate zone classifications. It discusses the development and application of the Köppen classification system and its connections to extreme weather events, LULC, and NDVI change. The findings could support the timely monitoring of extreme rainfall events utilizing remote sensing and reanalysis datasets. Furthermore, understanding how terrestrial vegetation responds to extreme weather events might have implications for the micro-level of the Himalayan mountains.

2. Study region

Sikkim is a state in northeastern India recognized for its distinct terrain. Sikkim's peculiar topography and climate have influenced its history, culture, and economy, making it a compelling and diverse region. The significant elevation variation in the Sikkim Himalaya (e.g., India), ranging from 300 m to 7000 m,

has profound implications for the local climate and the study of the region. This diverse topography influences the formation of distinct climatic zones, leading to typical cold, snowy winters and warm summers, characteristic of an alpine climate as per the Köppen classification^[33,34]. The varying elevations contribute to the complexity of the region's climate patterns, affecting agricultural practices, water availability, and local livelihoods^[34,35]. Additionally, the elevation gradient plays a crucial role in the distribution of glacial and high-altitude lakes, impacting the potential for glacial lake outburst floods and necessitating continuous monitoring due to climate change-induced glacier melting^[36]. Understanding the implications of elevation differences is vital for assessing climate vulnerabilities, adaptive capacities, and sustainable development strategies in the Sikkim Himalaya (**Figure 1a**). The political boundary separates it into six districts, Mangan previously called north Sikkim. Others are Gangtok, Pakyong (as east Sikkim), Namchi (as south Sikkim), Soreng, and Gyalshing or Geyzing (as west Sikkim). The streams and tributaries of the Teesta River have a complex network over the entire Sikkim region until its confluence downstream into the Rangit River (**Figure 1a**). The springs and streams are the major source of the Drinking water in Sikkim. On the basis of the Köppen classification Dash et al. (2012) have suggested that there are typical cold, snowy winters and warm summers in the state of Sikkim, which have an alpine climate^[37]. The climatic classes in the Sikkim Himalaya are crucial due to the significant impact of global climate change on the region's environment and human activities^[36,37]. The changing climatic factors have led to the enlargement of glacier-fed lakes, posing a threat to downstream communities in case of breaches^[38,39]. Additionally, rising global temperatures and altered rainfall patterns are affecting the glaciers that feed the rivers in the Himalayas, leading to water stresses in a region known for its water abundance^[40,41]. These environmental changes are accelerating cryosphere thawing, resulting in the formation of new lakes and the expansion of existing ones, increasing the potential for glacial lake

outburst floods and highlighting the urgent need for monitoring and adaptation strategies to mitigate the impacts of climate change in the Sikkim Himalaya.

Moreover, in this study classification has been computed for a 42-year long-term period using the Köppen classification system with temperature and precipitation data (**Table 1**). Three classes have been found for such a long period. These are ETc, Cfb, and Cfc (**Figure 1b**). That explains ETc for cold, tundra, and cool summer climate; Cfb for moderately warm, humid, and warm summer climate;

and Cfc for moderately warm, humid, and cool summer climate zone (**Table 2**). The temperature for the measured automatic weather station (AWS) and ERA5-Land for the monthly average of 2021–2022 has been shown in the supplementary figure (**Figure S1**). This shows limitation (underestimation) in the ERA5-Land dataset over the Indian Himalaya ^[42–44]. There are 8 AWS stations that lie in different climatic zones, three in the north Sikkim (ETc) zone, two in the east, and three in the south Sikkim (Cfb) zone.

Table 1. The details of the dataset used in the present study.

Variable used	Data type	Period	Resolutions		Source	Reference
			Spatial	Temporal		
T (2 m air temperature)	ERA5-Land (gridded)	1980–2021	$0.1^\circ \times 0.1^\circ$	Hourly	ECMWF	Muñoz-Sabater et al., 2021
P (total precipitation)						
LULC	Landsat-5, 7, 8, 9 (raster)	1989–2021	30 m	Once at a time	USGS EarthExplorer	Masek et al., 2006; Vermote et al., 2017
NDVI						
Topography	ASTER- GDEM-003 (DEM)	2011	30 m	2011	USGS EarthExplorer	Meyer et al., 2011
Population density	Population GPWv4 (gridded)	1990–2020	30 arc-second	for every five years	NASA (SEDAC)	Warszawski et al., 2016

Source: Muñoz-Sabater et al. ^[45–49].

Table 2. Criteria for Köppen climate classification.

Climate class	Name	Attributes
A	Tropical humid climate	Lowest $T_{\text{mon}} > 18^\circ\text{C}$
B	Dry climate	Dry boundary (boundary toward forests) is: for the precipitation period in winter: $P_{\text{annual}} < 2 T_{\text{annual}}$ for fuzzy precipitation: $P_{\text{annual}} < 2 T_{\text{annual}} + 14$ for the precipitation period in summer: $P_{\text{annual}} < 2 T_{\text{annual}} + 28$
C	Moderately warm climate	The lowest T_{mon} is between 18°C and -3°C
D	Moderately cold climate	Highest $T_{\text{mon}} > 10^\circ\text{C}$, and the lowest $T_{\text{mon}} < -3^\circ\text{C}$
E	Cold climate	Highest $T_{\text{mon}} < 10^\circ\text{C}$
Type	Name	Attributes
S	Steppe climate	The boundary between the steppes and the deserts are: for the precipitation period in winter: $P_{\text{annual}} = T_{\text{annual}}$ for fuzzy precipitation period: $P_{\text{annual}} = T_{\text{annual}} + 7$ for the precipitation period in the summer: $P_{\text{annual}} = T_{\text{annual}} + 14$
W	Desert climate	$P_{\text{annual}} < 250 \text{ mm}$
f	Humid climate	No dry season
m	Monsoon climate	The rainy period compensates for the scarcity in the dry season
s	Dry summer	Summer is the driest season
w	Dry winter	winter is the driest season
T	Tundra climate	The highest T_{mon} is between 0°C and 10°C
F	Climate of the eternal frost	Highest T_{mon} below 0°C

Subtype	Name	Attributes
h	Hot climate	$T_{\text{annual}} > 18^{\circ}\text{C}$
k	Cold climate	$T_{\text{annual}} < 18^{\circ}\text{C}$, and the highest
a	Hot summer	Highest $T_{\text{mon}} > 22^{\circ}\text{C}$
b	Warm summer	Highest $T_{\text{mon}} < 22^{\circ}\text{C}$, and least
c	Cool summer	Less than 4 $T_{\text{mon}} > 10^{\circ}\text{C}$, and the lowest $T_{\text{mon}} > -38^{\circ}\text{C}$
d	Very cold winter	Lowest $T_{\text{mon}} < -38^{\circ}\text{C}$

Source: Adopted after Milovanović et al., 2017^[50].

Note: T_{mon} : mean monthly temperature; T_{annual} : mean annual temperature; P_{annual} : the amount of precipitation.

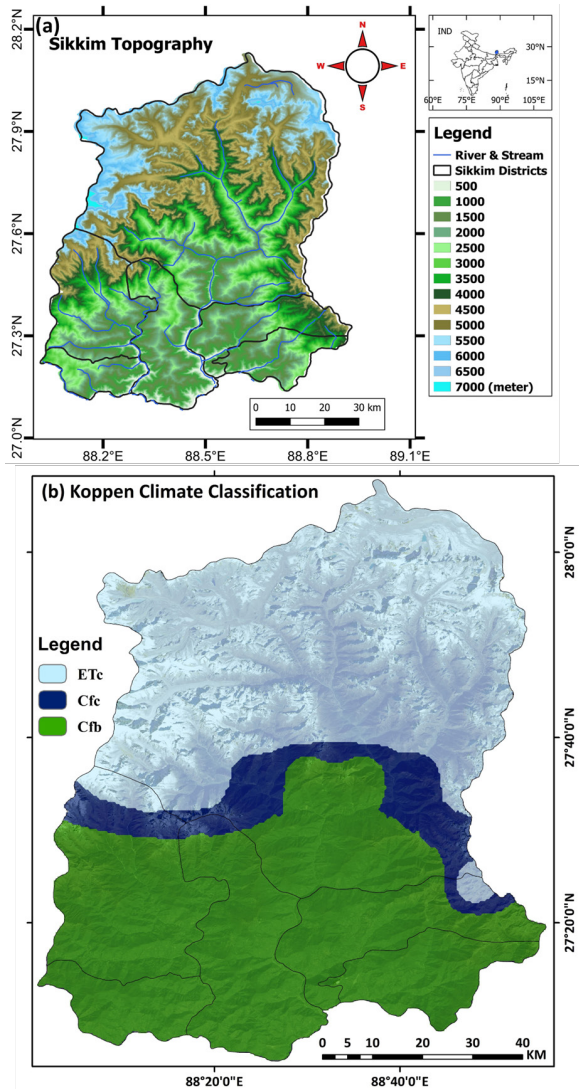


Figure 1. (a) Topography, stream, and river of Sikkim Himalaya, (b) Köppen climate classification for 1980–2021, and Landsat-9 image of 2021 (in the background).

3. Data and methods

The various data sets utilized in this study are

important in a broad aspect of environmental and climatological investigations (**Table 1**). The NDVI dataset provides essential information for assessing ecosystem health and dynamics. The land use land cover (LULC) data is an essential tool for land use planning, urban growth forecasting, and climate controls. Its monitoring relies heavily on remote sensing imagery. Temperature measurements have applications for investigating the impacts of climate change. Hydrometeorological evaluations require precipitation records, which emphasizes the significance of choosing relevant data with different geographical and temporal resolutions. Furthermore, the Köppen classification contributes to regional climate evaluations and a greater understanding of climate trends and categories. The significance of each dataset to the many study goals; which ranged from vegetation analysis to land cover change, effect evaluations of climate change, and investigations into precipitation variability, was taken into consideration while adopting data. The methods for all points are discussed in the subsections below:

3.1 NDVI calculation

The Normalized Difference Vegetation Index (NDVI) is a remote sensing technique that measures the health and abundance of vegetation. This is computed by deducting the reflectance of red light from that of near-infrared (NIR) light and dividing it by the sum of these reflectances. The following calculation normalizes the variances within the two bands, producing a number between -1 to $+1$. The present study uses various data sets for the analysis (**Table 1**). The calculation of NDVI has been conducted for the

years 1989 and 2004 using Landsat (LT) 5 (Band 3 & 4), and for 2021 using LT 9 (Band 4 & 5). The acquired LT Collection 2 Level 2 (C2L2) 16-bit unsigned images were processed to derive surface reflectance values within the range of 0 to 1. Subsequently, the NDVI was computed for each respective year. Notably, glaciers and snow cover exhibit very low NDVI values, while areas with thriving vegetation exhibit high NDVI values^[51–53]. To identify areas of high recent to old i.e., post to pre-changes, differential NDVI (dNDVI) is calculated^[54,55]:

The differential NDVI was calculated as,

$$\text{dNDVI} = \text{NDVI}_{(\text{Post})} - \text{NDVI}_{(\text{Pre})} \quad (1)$$

Using the equation dNDVI was calculated between the years 1989, 2004, and 2021 (**Figure 2**).

To evaluate the health of the vegetation and track changes in its cover, the NDVI and its change over time (dNDVI) are essential measures. NDVI, which is produced using satellite data such as Landsat and MODIS, offers important insights into the dynamics of vegetation over an extended period and makes it possible to identify certain seasonal and regional trends. Research has indicated that seasons, land use, and climate all affect NDVI values. Precipitation is a major component in determining NDVI fluctuations in some areas. High-resolution NDVI chronology information can also be used to precisely supervise terrain to maximize vegetation productivity by highlighting the link between vegetation growth patterns and land characteristics. Moreover, dislocation and decline patterns in plant cover across time can be revealed by employing landscape metrics to analyze multitemporal NDVI observations. This is crucial for evaluating biodiversity and promoting sustainable landscape management.

3.2 LULC classification

Land use land cover (LULC) denotes the physical composition and features of the Earth's surface, which includes both human-induced activities and natural components. This is a fundamental concept in satellite imagery and geographic information

systems for analyzing and regulating anthropogenic and natural environmental effects on landscapes. The process of LULC classification is essential to comprehending and managing the environment. This includes categorizing the surface of the Earth into various classifications according to human as well as natural interaction. The usefulness of LULC classification in terms of growth, urban planning, environmental management, and climate change study is precisely what makes this method significant. The analysis encompasses the spatial and temporal variabilities in LULC, spanning from 1989 to 2021. To achieve this, an iso cluster unsupervised classification technique was employed on Landsat (LT) Collection 2 Level 2 (C2L2) images^[56–58]. The iso cluster unsupervised classification technique, as described, uses techniques for clustering such as maximal likelihood classification to process Landsat images for environment monitoring. This approach attempts to categorize pixels into discrete land cover classes such as bare soils, watersheds, forests, ice-covered regions, and others, adding to nature conservation and sustainable development efforts in locations like Sikkim.

The iso cluster is a powerful classification technique, widely used for mapping land use and land cover types, monitoring environmental changes, and assessing damage after natural disasters^[57,58]. The study focused on utilizing C2L2 data from various LT satellites: LT 5 for 1989, 1994, 2004, and 2009; LT 07 for 2000; LT 08 for 2015; and LT 09 for 2021 within the state of Sikkim. Data acquisition occurred in December for all years except for 2004, where data from November was utilized. Additionally, data selection ensured that the imagery contained less than 10% cloud cover. The classification approach was employed to categorize Sikkim's LULC into five distinct classes: forests, barren land, and scattered built-up areas, talus slopes and debris, glacier geomorphs, and glaciers and snow (**Figures 3 and 4**).

3.3 Climate variability analysis

For Köppen classification, temperature and precipitation daily data have been used for 1980-2021.

The ERA5-Land dataset is gridded and covers the entire globe. However, we have utilized it for Sikkim. Furthermore, the daily data has been converted to the long-term monthly average for the Köppen classification. However, for extremely wet days, daily precipitation is used. We computed wet days (daily precipitation greater than 1mm, i.e., $P \geq 1\text{mm}$) and then the 99th percentile using 1961–1990 precipitation as a reference period. However, precipitation anomaly from the long-term average has been computed for each year 1990–2020, to see the anomalous behavior of the annual precipitation over the region. For climate variability, the study period has been divided into four decades D1: 1980–1990; D2: 1991–2000; D3: 2001–2010; and D4: 2011–2021. The corresponding decades' temperature change (ΔT_{Dn}) and precipitation percentage change ($\Delta P_{Dn}(\%)$) have been computed as Equations (2) and (3).

$$\Delta T_{Dn} = \left\{ \left(\frac{\sum_{t0}^{t10} T_n}{10} \right) - \left(\frac{\sum_{t0}^{tm} T}{m} \right) \right\} \quad (2)$$

$$\Delta P_{Dn}(\%) = \left(\frac{P_{Dn} - \bar{P}}{\bar{P}} \right) \times 100 \quad (3)$$

where $\bar{P} = \left(\frac{\sum_{t0}^{tm} P}{m} \right)$, and $P_{Dn} = \frac{\sum_{t0}^{t10} P}{10}$, the 'n' is the number for the corresponding decades (as D1, D2, D3, and D4), and 't' is the time period for the decades. The investigation of precipitation changes over several decades provides useful insights into shifting rainfall patterns. Several reasons contribute to these patterns, including regional climatic systems, global warming, and internal mechanisms of climate variability such as ISM, ENSO, and IOD. The 'm' is the complete period (1980–2021) of the study. Equations (2) and (3) are used for the decadal variability of the climate system over the entire Sikkim. as output is visualized as temperature vs precipitation change.

The significant change has been assessed using a one-tailed t-test as the t-test^[59] has been applied for the significant difference and trend values as Equation (3).

$$t\text{-test} = \frac{(\bar{D}_2 - \bar{D}_1)}{\sqrt{\left(\frac{\sigma_1^2}{n_1} + \frac{\sigma_2^2}{n_2} \right)}} \quad (4)$$

where (\bar{D}_1) , (\bar{D}_2) , σ_1 , σ_2 , and $n_1 = n_2 = 10$ years are the mean of first-time D1 (from 1980 to 1990) of the variables, means of second-time series D2 (from 1991 to 2000) (similarly for D3 and D4) standard deviation for the first decade D1, standard deviation for the second decade D2, total number years for the first decade 1980 to 1990 (11 years), and total number of years for the second decade 1991 to 2000 (10 years), respectively for D3 and D4. This is used to find the p-values and significant investigation with a p-value table^[60].

The Mann-Kendall test is a popular non-parametric tool for trend estimation in a variety of domains, especially climatology and hydrology. It is used to find monotonic trends in time series, like precipitation patterns or temperature, by determining whether there is a constant increase or decrease over time^[61]. However, the Mann-Kendall test has limitations, such as the requirement for serially uncorrelated data to minimize errors in determining trends^[62]. To address this, pre-whitening approaches have been devised to reduce autocorrelation effects while improving test performance^[63]. The Mann-Kendall trend analysis^[64,65] is made for the assessment of rising and declining patterns of extremely wet days over the entire Sikkim. This is important to divide the study period into decades since this enables a more thorough examination of long-term trends and fluctuations in variables like temperature and rainfall. This approach presents important insights for sustainable planning and decision-making by assisting in the identification of trends, changes, and possible effects throughout time. Because the Mann-Kendall trend analysis is a useful statistical test for identifying monotonic trends in time series data, it certainly makes it reasonable to apply this technique.

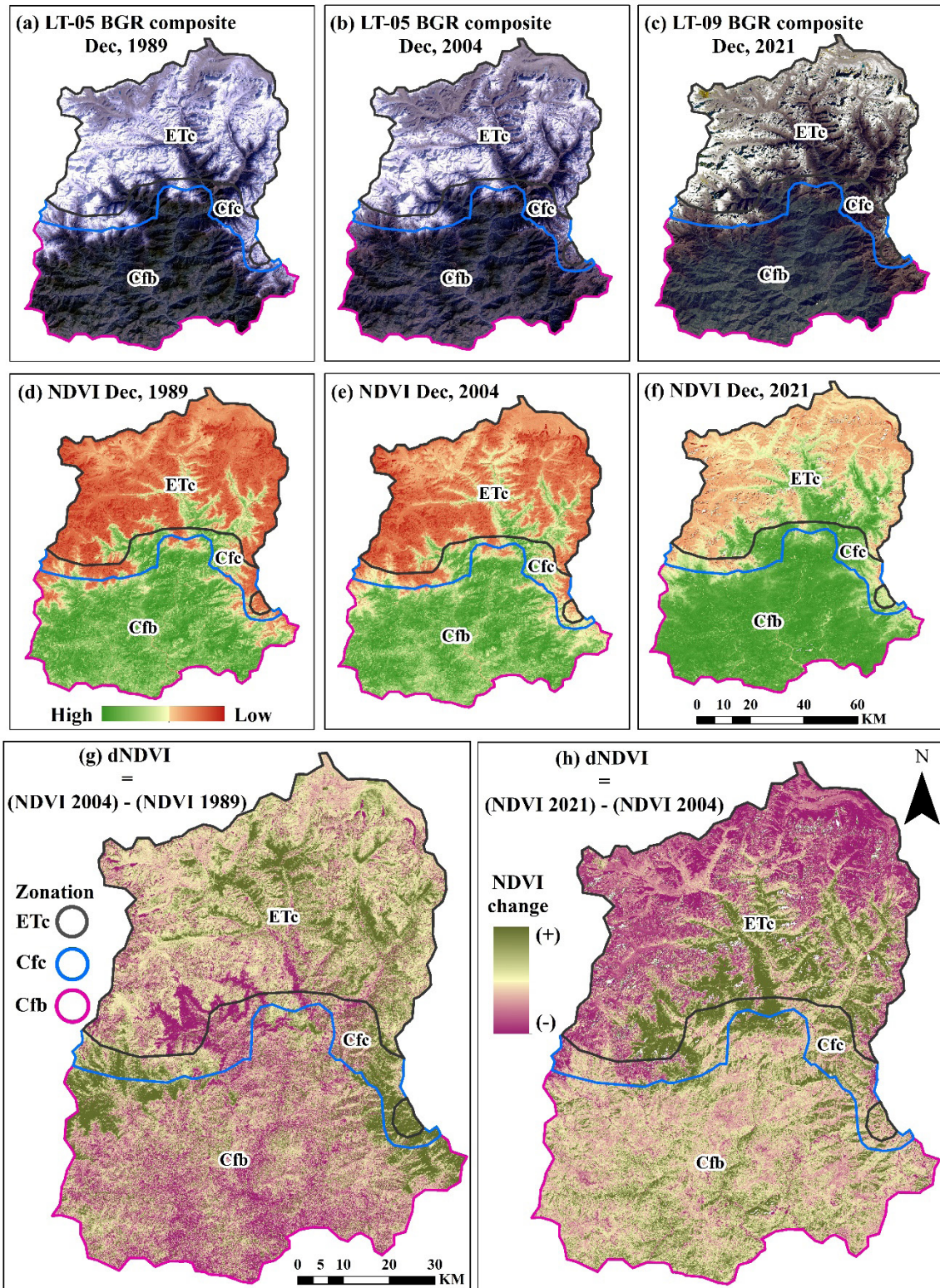


Figure 2. Normalized Difference Vegetation Index (NDVI) and change of four decades (1980–2021) over the Sikkim (Landsat 5 and 9).

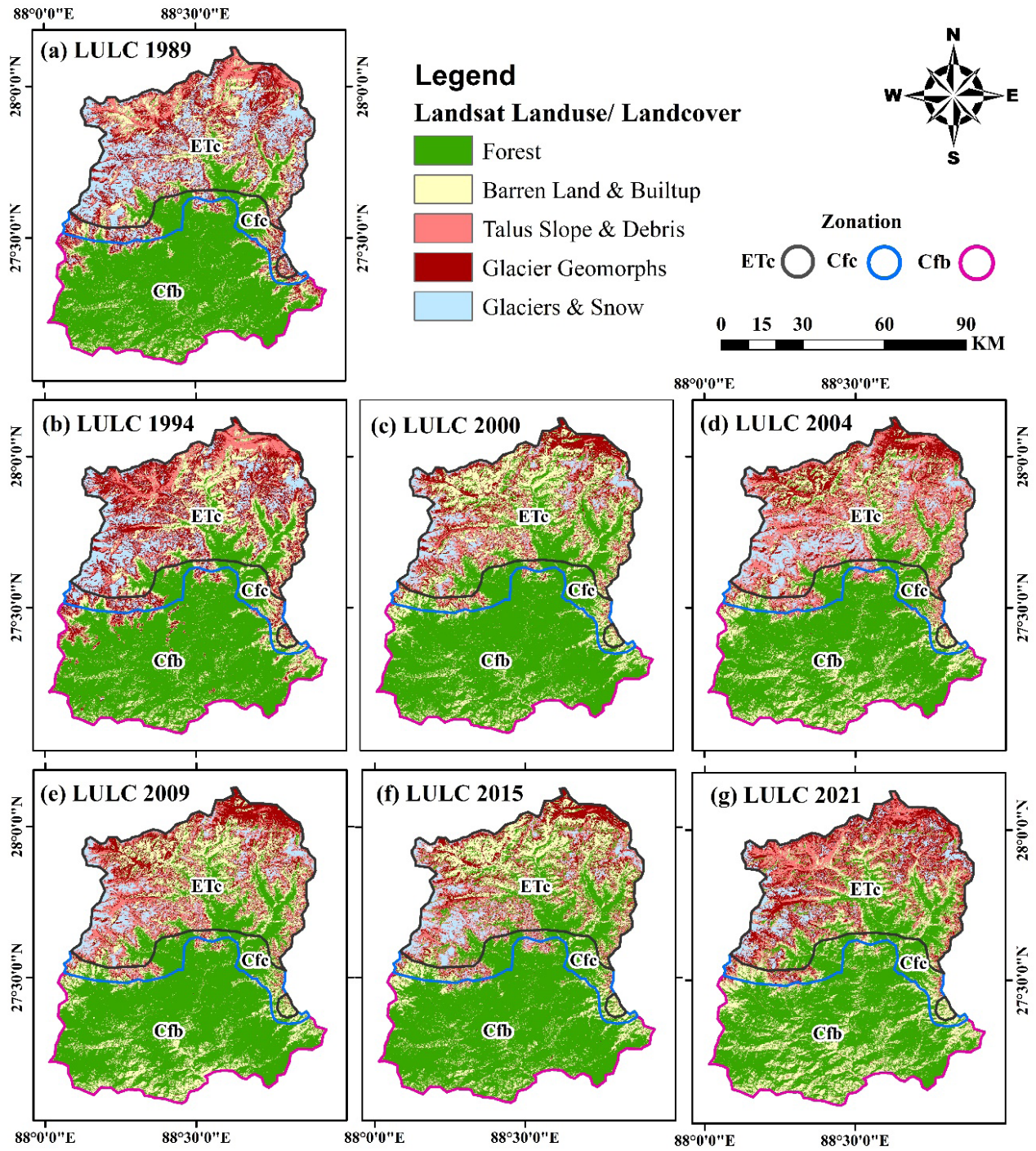
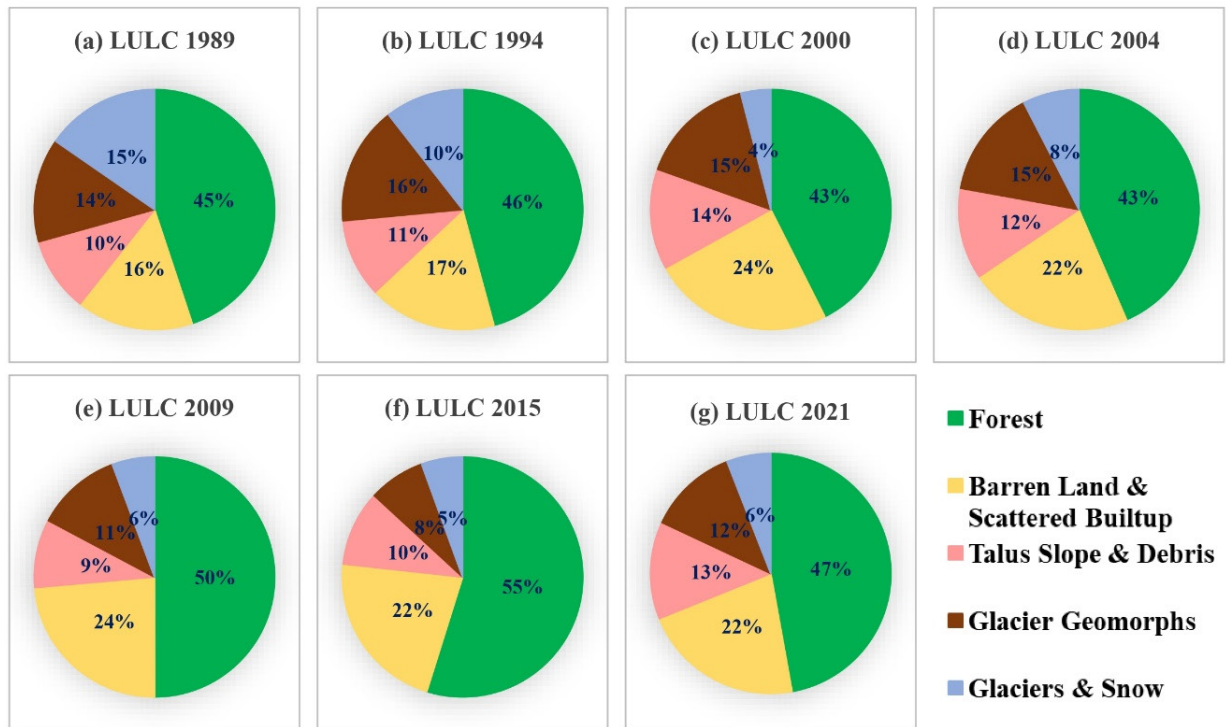


Figure 3. Land Use Land Cover (LULC) for the study period (1980–2021) of the available dataset (Landsat-5, 7, 8, and 9).



LANDUSE/ LANDCOVER (1989 - 2021)

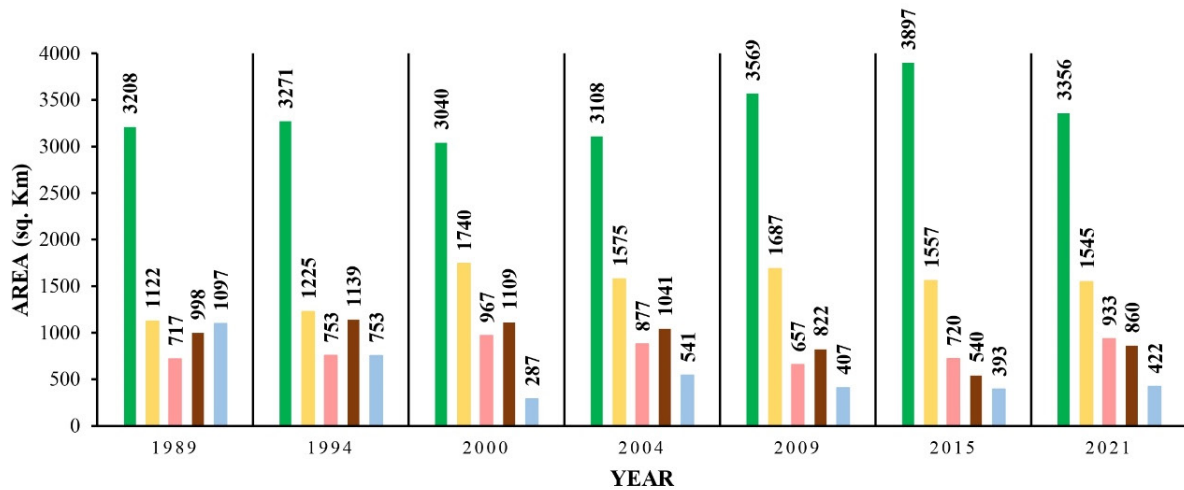


Figure 4. Land Use Land Cover (LULC) (percentage change) for the study period (1980–2021) of the available dataset Landsat-5, 7, 8, and 9 over the entire Sikkim.

4. Results

4.1 NDVI change

Figure 2 shows the NDVI for different years and changes for 2004–1989 and 2021–2004. Analysis of NDVI data from 1989, 2004, and 2021 reveals a significant expansion of vegetation cover to higher altitudes (**Figures 2a–2h**). Areas that were previously covered by snow and devoid of vegetation are now occupied by shrubs and grasslands. The contrast in change is relatively minor between the years 1989 and 2004 (**Figures 2d** and **2e**).

However, a considerable change is evident from 2004 to 2021; vegetation has distinctly encroached upon the elevated regions of the northeastern and central-northern parts of the state (**Figures 2e** and **2f**). Furthermore, the NDVI study confirms the decrease and loss of snow cover in the state's southeast regions, which was determined by the LULC classification.

In the year 1989 (**Figure 2d**), the southeastern corner was characterized by snow cover, as reflected by very low NDVI values. NDVI values gradually increased in 2004 (**Figure 2e**) and considerably more in 2021 for this specific area (**Figure 2f**), indicating a decrease in snow cover and subsequent vegetation encroachment^[40]. The observation indicates that in the studied area when the snow cover diminishes and the previously covered land becomes exposed and barren, there is a shift in the NDVI value from the negative to the positive side. Between the years 1989 and 2004, the dNDVI reveals a significant and pronounced negative change in the western central and southern regions of the state (**Figure 2g**).

This indicates instances of degradation or loss in vegetation cover in the southern regions, which is noticeable in the LULC classification (**Figures 3a–3g**). The classification reveals a 6% rise in barren land and sparsely distributed built-up areas, along with a 2% and 7% reduction in the forest and snow cover of Sikkim (**Figure 4**). On the other hand, a strong negative dNDVI at parts of central northwestern Sikkim is attributed to positive snow coverage between 1989 and 2004 in this specific area. The 6 % increase

in Barren land and built-up (**Figures 4a–4g**) is also associated with the positive dNDVI at the southeastern corner where the previously snow-covered area changed to Barren rugged topography. Other areas of positive dNDVI and vegetation encroachment to snow-covered areas are the central west, central north, and northeastern part of mountains (**Figures 2g** and **2h**).

The dNDVI analysis spanning from 2004 to 2021 reveals notable changes primarily observed in the northern, northeastern, and northwestern regions of the State (**Figures 2g** and **2h**). The rise in vegetation density in the central northeastern area of Sikkim is evident from the positive values of dNDVI (**Figures 2g** and **2h**). This aligns with the earlier LULC classification, which demonstrated a 4% augmentation in vegetation cover (**Figures 4a–4g**). On the other hand, the negative dNDVI values in the northern mountain ranges of the state are linked to a 2% reduction in snow cover, a 3% decline in glacier geomorphology, and a 1% increase in barren land (**Figures 4a–4g**).

4.2 LULC change

Figure 4 shows the percentage and area of the various classifications in different years for the entire Sikkim. Sikkim, situated amidst harsh climatic conditions, particularly in its northern and western regions due to elevated mountains and glaciers, experiences a challenging environment. As a result, a significant portion of the state is composed of glacier geomorphology and permafrost-related talus slopes and debris^[56–58]. Given the context of shifting climatic patterns and the diminishing cryosphere, this classification scheme places heightened emphasis on the interconnected aspects of climate and landform variations. The forest cover within the state displays minimal fluctuations throughout the study period, ranging from 43% to 55%. Specifically, the forest cover accounted for 45% of the total area i.e., 3208 sq. km in 1989, and maintained at 47% i.e., 3356 sq. km in 2021 (**Figures 4a–4g**).

The most extensive forest cover was observed in 2015 i.e., 55%, while the lowest was noted in

2000, and 2004 i.e., 43% (**Figures 4d–4g**). It's important to note that the classification incorporates all forms of vegetation under the “forest” category. Consequently, there's a possibility that changes in various vegetation types over the period might have been overlooked in the results. Blue, Green, and Red (BGR) composite images from the LT satellite reveal that significant portions of the higher-altitude northern and north-western regions of the state have experienced an increase in scattered vegetation cover in recent years (**Figures 2a–2c**).

The expanse of Barren Land and Built-up areas within the state has exhibited a steady increase over the studied timeframe. This category encompassed 16% of the total area i.e., 1122 sq. km in 1989, and by 2021, it had expanded to cover 22% of the region i.e., 1545 sq. km (**Figures 4a–4h**). The increase in barren land has notably stood out in the northern regions of the state, while the expansion of built-up areas has become evident in multiple dispersed urban clusters across the state, primarily concentrated in the southern, south-eastern, and south-western parts. A substantial rise in barren land has been particularly observed in the southeastern corner of the state in recent decades. This area of the state, previously blanketed by perpetual snow, has undergone a complete transformation, with the loss of snow resulting in the emergence of barren and rugged topography.

The presence of numerous and extensively distributed talus slopes and debris-covered regions within the state indicates a decline in permafrost due to climate change. This particular LULC class also demonstrates an expansion from 10%, equivalent to 717 sq. km, to 13%, covering 933 sq. km, over the duration of the study (**Figure 4h**). Talus and debris slopes are significant features in the high-altitude mountainous areas of Sikkim. The increased coverage of this class holds implications for the reduction of permafrost, heightened erosion processes, and other related effects. Unstable debris slopes could potentially pose a risk of stream or river blockages in certain areas, leading to the formation of artificial lakes, which, in turn, negatively impact ecological aspects and elevate hazard vulnerability downstream.

Glacier geomorphology constitutes a significant portion of the northern and north-western regions of the state. This specific LULC category consistently occupied an area of 14% to 15% of the total land area from 1989 to 2004.

Subsequently, there was a decline in coverage, reaching 8% in 2015. As of 2021, glacier geomorphology encompasses 860 sq. km, equivalent to 12% of Sikkim's total area (**Figure 4h**). This class primarily includes elongated stretches of debris-covered glaciers and moraines. The reduction in coverage in this category signifies a decrease in the extent of debris-covered glacier tongues. This observation is reinforced by the concurrent increase in the area classified under the talus and debris slope category.

4.3 Climate zonation with climatic variability

The class with the most consistent reduction in area is glaciers and snow. In order to ensure unbiased observation of its changes, all LT images used for the analysis were taken in the month of December, except for the year 2004 when they were acquired in November. In 1989, glaciers and snow occupied an area of 15%, totaling 1097 sq. km.

By 2000, this snow and glacier coverage decreased to 4%. As of the most recent year, 2021, glaciers and snow now encompass an area of 422 sq. km, accounting for 6% of Sikkim's total land area. The reduction in the cryosphere's extent is noticeable in the LT BGR composite imagery as well. During the period from 1989 to 2004, the south-western, south-eastern, and north-eastern parts experienced a decline in snow cover. Conversely, lower-altitude southern, eastern, and south-western areas have witnessed a reduction in densely forested regions. Therefore, the apparent lack of notable variation in overall forest or vegetation cover between 1989 and 2021 in Sikkim could be attributed to the compensatory growth of high-altitude grasslands counterbalancing the loss of dense forests in lower-altitude populated regions. Especially southern part of Sikkim (i.e., Gangtok, Pakyong, Namchi, Soreng, and Gyalshing or Geyzing) has a notable change in population from 1990 to 2020 (**Figures S2 and S3**). That

is the Cfb climate classification zone favorable for thriving human life, however, in recent decades this climatic zone has been facing significant warming (Figures S4 and S5), especially the southern tip of the study region. Moreover, new climate types (Efc and Cfa) intrusion in the southern part of the zone have been observed (Figure 5). All grids of the study region have altered from cold-dry to warm-wet from

D1 to D4 (Figure 6).

Climate change-induced glacier and snow cover loss in Sikkim jeopardize local ecosystems and water resources. Sikkim's decreasing snow cover and increased debris and glacier lakes have disturbed the regional climate balance, affecting daily mountain lifestyles and farming methods. The Sikkim Mountains have shown that glacial retreat and snow

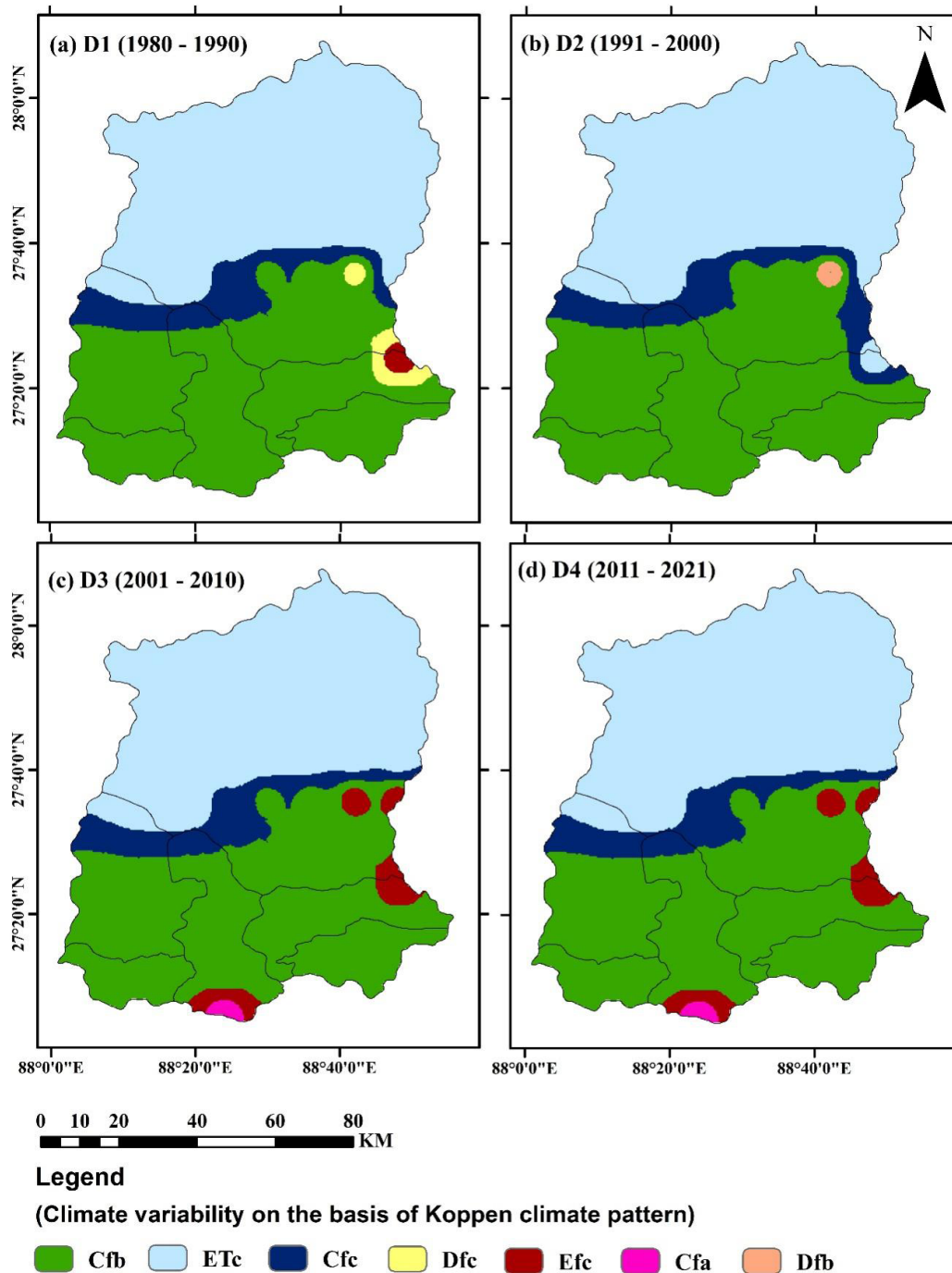


Figure 5. Climate variability for four different decades (1980–2021) as D1, D2, D3, and D4, based on the Köppen climate pattern.

loss restrict runoff, influencing reservoirs and the availability of streams. Furthermore, the production of glacial lakes due to glacier shrinkage is a serious concern, with the number of glacial lakes increasing rapidly over decades, representing potential catastrophic risks and dangers to the region's topography and water supplies ^[66].

However, significant changes were observed in the major glaciated region located in the north-western part between the years 2004 and 2021. The warming over the entire Sikkim has been evidenced from -0.6°C to $+0.8^{\circ}\text{C}$ with respect to precipitation raised from -10% to $+18\%$ from the first decade (1980–1990) to the recent decade (2011–2021) (Figure 6). This justifies the significant changes observed in the major glaciated region. The anomalous high precipitation in recent two decades, mostly over the southern part of the state is indicating to rising trend of extremely wet days (Figures 7 and 8). The opposite for the northern district (i.e., Mangan) has been witnessed (Figures 7–9).

Figure 8 represents the spatial distribution of extremely wet days annually over Sikkim. The extreme wet days over the central part of the Sikkim (i.e., upper part of the Cfb climate zone). Figure 9 suggests the precipitation change in different decades, the first two decades difference D2 and D1 (Figure 9a) shows a negative change in the precipitation with a small portion of the region on significance over the southern part of the Sikkim. But, a strong positive over the northern part of the state. Furthermore, for the recent two decades difference between D4 and D3 (Figure 9b) shows significantly positive change over the entire Sikkim (except northernmost having insignificantly negative). Figure 9c shows the spatial distribution of trends in extremely wet days for the study period (1980–2021). The negative trend has been found over the entire northern part (ranges from -0.04 to -0.1) but the southern part has a positive trend value ranging from 0.06 to 0.1 day/year. It is also observed that the temporal trend of extremely wet days is declining (Figure S6).

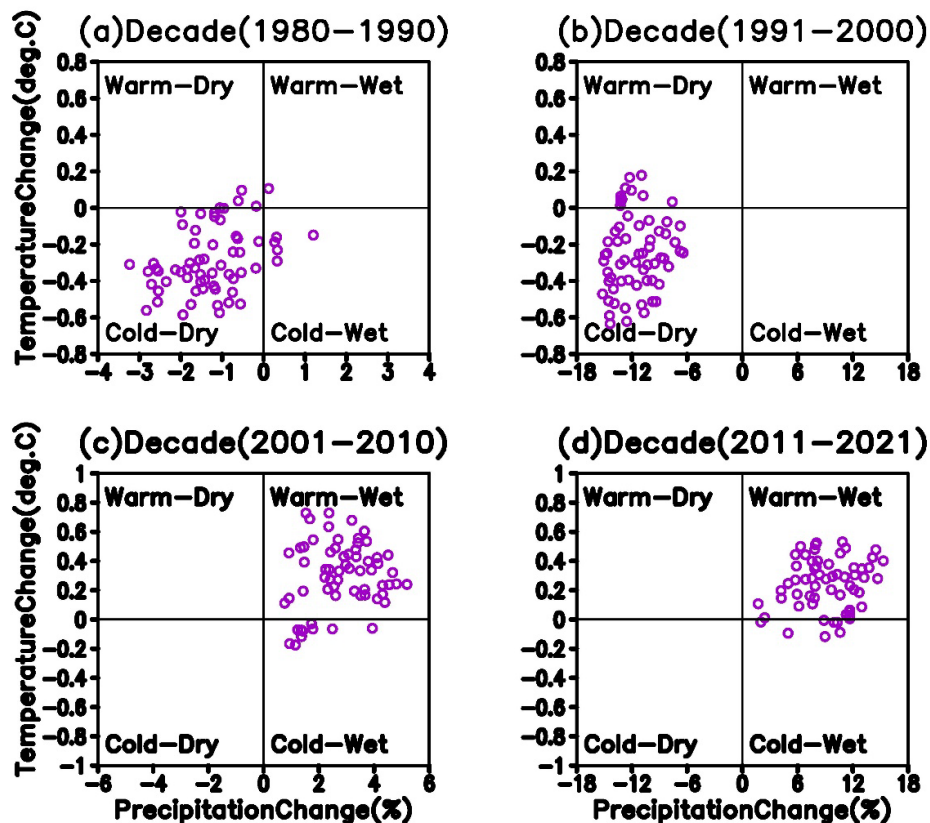


Figure 6. The climate variability based on temperature and precipitation change concerning 1980–2021 over the entire Sikkim Himalaya (here each point represents one grid of the region) using ECMWF, ERA5-Land dataset.

Understanding and resolving Sikkim's trends is critical not only for local people but also for larger attempts to mitigate the effects of climate change globally. The observed patterns in Sikkim show the importance of adopting preventive steps to ensure

long-term agricultural practices and water resource management in the face of changing climate scenarios^[67]. The elevation-dependent warming in the Sikkim Himalaya is also affected by global climate change^[41].

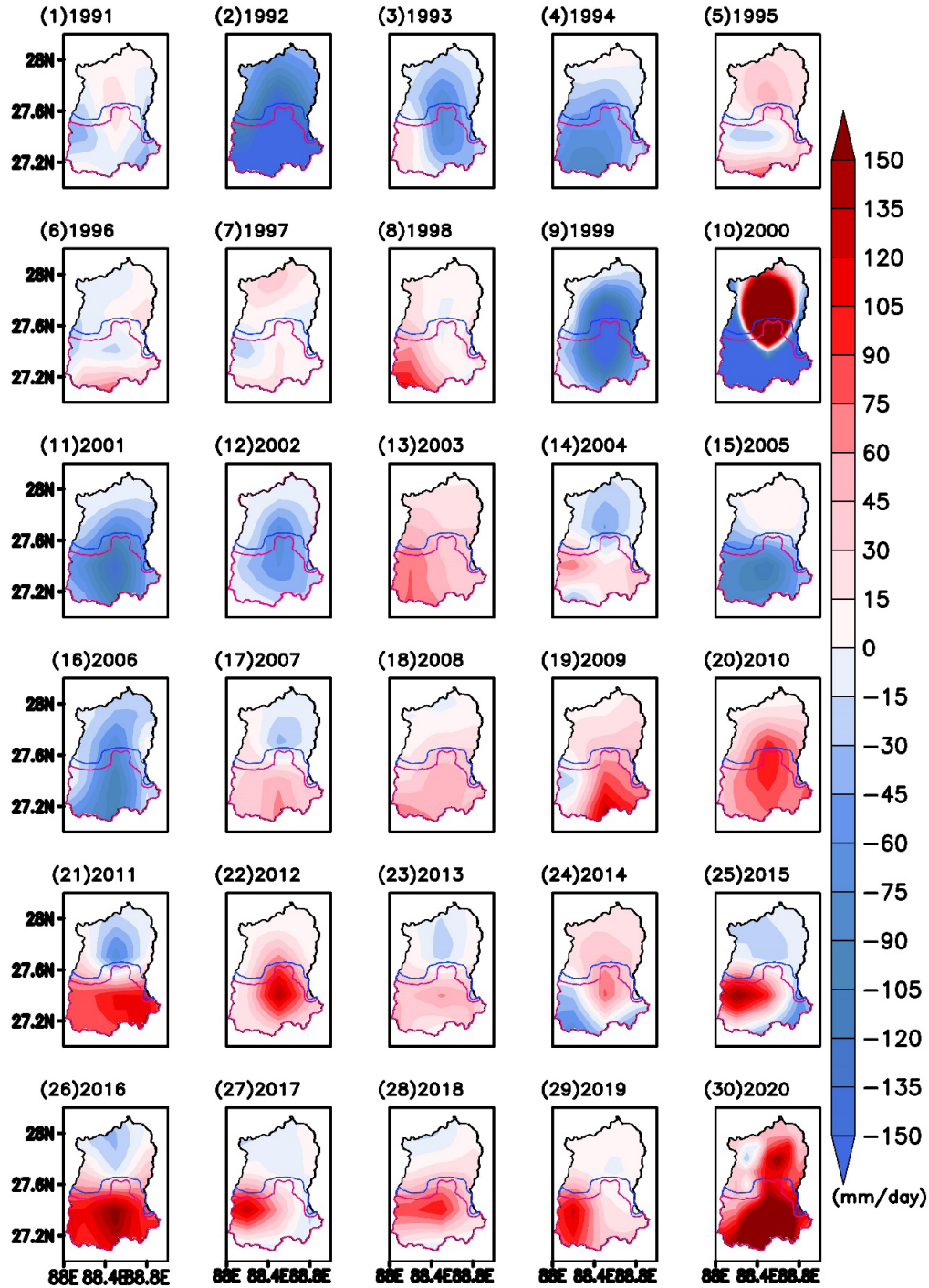


Figure 7. Spatial distribution of total precipitation anomaly from the long-term mean (1980–2021) for the study period over Sikkim using ECMWF, ERA5-Land dataset. The lines represent the climatic zonation 'black for ETc', 'blue for Cfc', and 'magenta for Cfb'.

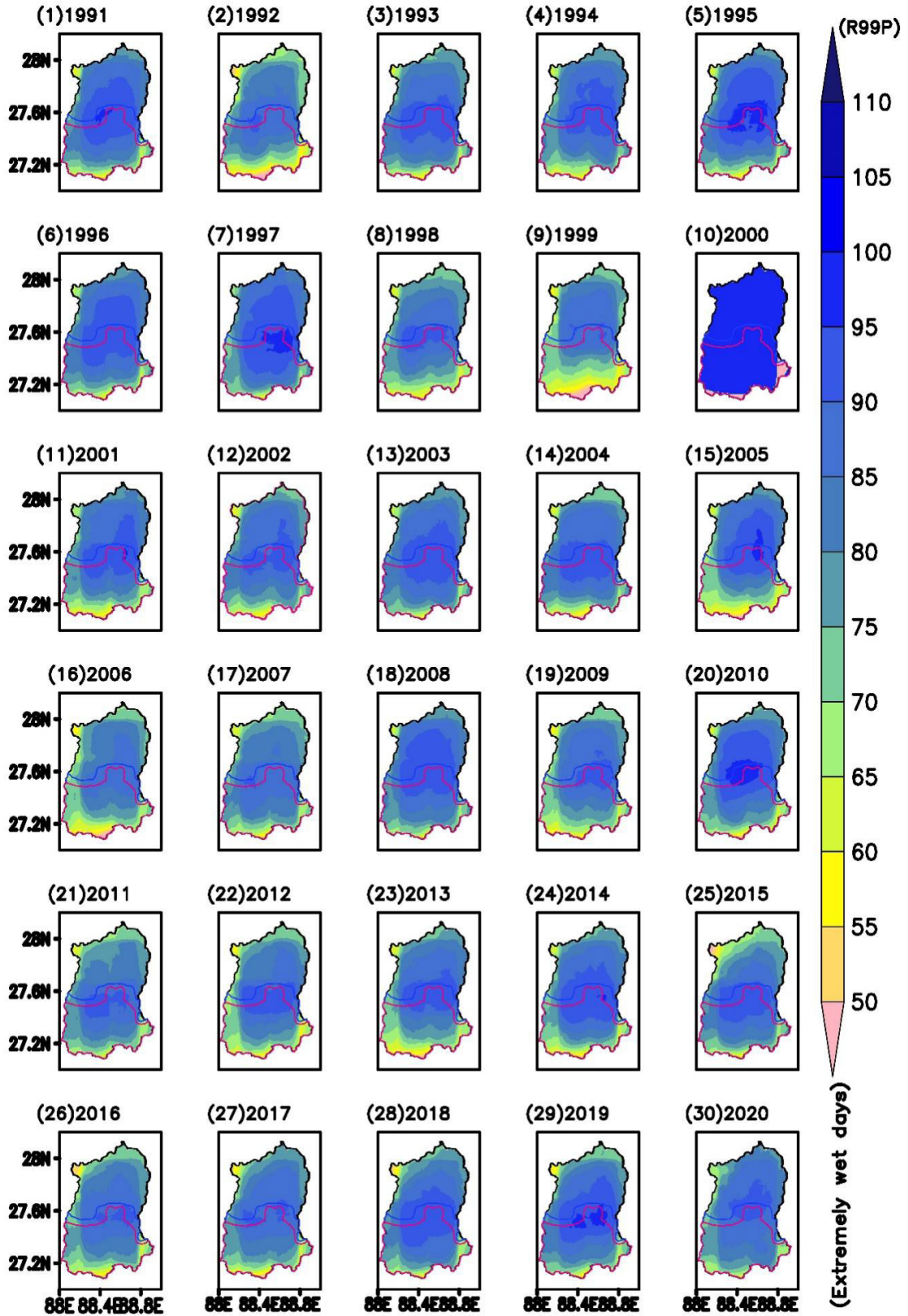


Figure 8. Extremely wet days for the study period with reference to 1961–1990 using ECMWF, ERA5-Land dataset. The lines represent the climatic zonation ‘black for ETc’, ‘blue for Cfc’, and ‘magenta for Cfb’.

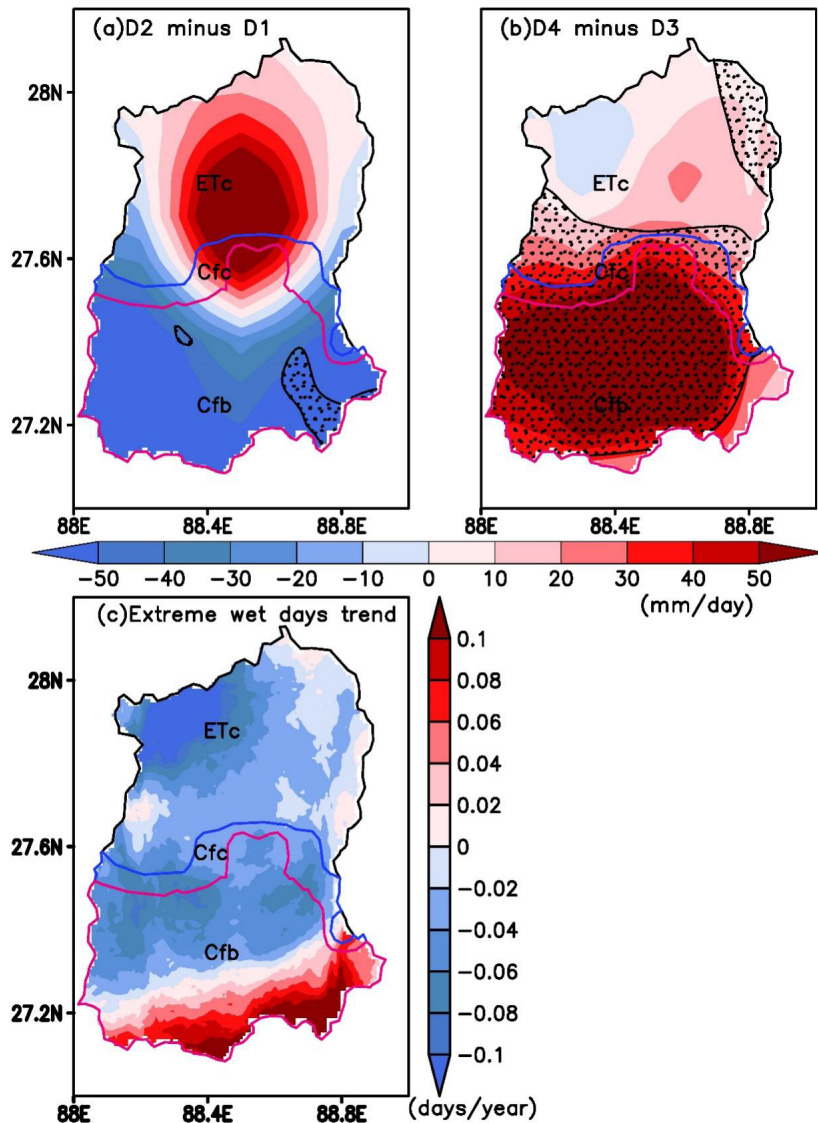


Figure 9. Total precipitation change (dots represent 95% significance level) in (a) past decade D1: 1980–1990; D2: 1991–2000, and (b) recent decades D3: 2001–2010; D4: 2011–2021. (c) the linear trend of extremely wet days for a long period of time (1980–2021) using the ECMWF, ERA5-Land dataset. The lines represent the climatic zonation ‘black for ETc’, ‘blue for Cfc’, and ‘magenta for Cfb’.

5. Discussion

Sikkim’s challenging environment, with elevated mountains and glaciers, leads to diverse LULC patterns. Forest cover remained relatively stable throughout the study period, fluctuating between 43% and 55%^[68]. The apparent lack of significant variation in overall forest or vegetation cover might be due to compensatory growth of high-altitude grasslands counterbalancing forest loss in lower-altitude areas^[69,70]. Higher-altitude northern and north-western regions experienced increased

scattered vegetation, while lower-altitude southern and eastern areas saw reduced forested regions^[71,72]. Barren land and built-up areas expanded from 16% (1122 sq. km) in 1989 to 22% (1545 sq. km) in 2021. Extensively distributed talus slopes and debris-covered areas expanded from 10% to 13%. This expansion reflects a decline in permafrost due to climate change, with implications for erosion and hazard vulnerability downstream^[73]. Glacier geomorphology coverage decreased from 14%–15% to 8%, then increased to 12% in 2021. This change indicates a reduction in debris-covered glacier tongues, linked

to an increase in talus and debris slope areas^[68,74]. Glacier and snow coverage decreased significantly over the years, from 15% in 1989 to 6% in 2021. Notable changes were observed in various parts of the state, especially the major glaciated region in the northwest^[68,70,72]. The decrease in snow cover has led to the emergence of barren and rugged topography in previously snow-covered areas^[71,72]. Reduction in glacier and snow cover aligns with global trends of diminishing cryosphere due to anomalous warming and climate change^[75]. The climatic zone of eastern Gangtok (east Sikkim) especially the Nathula region has evidenced the microclimatic classification transformation from ETc, Cfc to Efc in the recent decades.

The analysis of NDVI data over the years reveals a significant expansion of vegetation cover to higher altitudes, especially in the northeastern and central-northern parts of the state^[68,70,76]. There's a minor contrast in change between 1989 and 2004, but a notable transformation from 2004 to 2021, suggesting an accelerated encroachment of vegetation onto elevated regions. The reduction of snow cover in the southeastern regions is not only evident through LULC classification but also reflected in the NDVI analysis. The study applies enhanced accuracy assessments of supervised LULC-classified remote sensing imagery. The supervised LULC-classification remote sensing imagery method widely applied is the least biased in terms of image classification and comprehension^[56]. The shift in NDVI values from negative to positive in the southeastern corner indicates that the decline of snow cover exposes the previously covered land, leading to the growth of vegetation^[71,72,76,77]. Between 1989 and 2004, negative dNDVI values in the western central and southern regions suggest significant degradation or loss of vegetation cover. From 2004 to 2021, positive dNDVI values in previously snow-covered mountainous northern, northeastern, and northwestern regions indicate notable increases in vegetation cover^[78]. The contrast in change is more pronounced in recent years (2004 to 2021) compared to earlier years (1989 to 2004), indicating potentially accelerated environmental changes. The decline of extremely wet

days is a consequence of anomalous warming over the mountainous region^[41,79]. Extremely wet days decline is directly linked to most of the precipitation occurrence in the shorter period of time^[41]. It can be seen from the recent decades' significant precipitation rise. Apparently understandable behavior of climate variability in the microclimatic region, the recent decades' significant precipitation has risen but at the same time, the extremely wet days have declined.

6. Conclusions

The current study determined three distinct climate classes (i.e., ETc, Cfc, and Cfb) in the Sikkim Himalaya based on the Köppen classification for the long term (42 years). Thus, it has been emphasized that the empirical basis of climate classifications, as well as the nature of data selection and the methodologies used to analyze climate variability and classification, are constraints on microclimatic zonation. Köppen classification system relies on precipitation and temperature data from various global datasets, highlighting uncertainties in climate types that could be due to dataset variations (AWS data as well). Over the entire Sikkim Himalaya, climate variability based on changes in temperature and precipitation from 1980 to 2021 comes to the conclusion that Sikkim's climate has changed from cold-dry to warm-wet (e.g., temperature rise from -0.6°C to $+0.8^{\circ}\text{C}$, percentage increase in precipitation from -10% to $+18\%$). In Sikkim, the effects of climate change on the environment and socioeconomics are devastating and multifaceted. Adequate policies for adaptation need to take into account the prospective near and long-term impacts of climate change and integrate community involvement, environmentally friendly practices, and reliable climate evaluating mechanisms.

Moreover, the Köppen climatic pattern from D1 to D4 is changing the regime with new classifications of Cfa, and Efc. The change in precipitation over the last two decades has been determined to be both negative in the past and notably positive in recent. Thereafter, extremely wet days are declining over

the entire ETc and Cfc climatic zones. Nevertheless, extremely wet days are rising over the southern part of the Cfb climatic zone. This suggests that temperature rise is the reason for the intense precipitation occurring more often within shorter periods, and urging the decreasing number of extremely wet days. The future implication of changing LULC scenarios for Sikkim to increasing pressure on land resources, driven by population growth and economic development. This could lead to further deforestation, biodiversity loss, and degradation of ecosystem services, necessitating proactive adaptation strategies focused on sustainable land management, biodiversity conservation, and climate-resilient development. The conclusions of this study performed in the Sikkim Himalaya will be useful in developing future strategies for environmental conservation, climate change adaptation, and sustainable development.

Author Contributions

Dr. Pramod Kumar: Conceptualization, analysis, figures, writing, editing, proof-read. Mr. Kuldeep Dutta: Analysis, figures, writing. Dr. Rakesh Kumar Ranjan: Continuous monitoring, mentoring. Dr. Nishchal Wanjari: Mentoring, and editing. Dr. Anil Kumar Misra: Mentoring.

Conflict of Interest

The authors declare that there is no conflict of interest.

Data Availability Statement

The data for the current study are publicly available as all are open-source datasets. However, the analyzed data will be available upon adequate request from the corresponding author.

Funding

This study received fellowship support for P.K. and K.D. from DST-CoE, Department of Geology, Sikkim University.

Acknowledgments

We acknowledge ‘DST-CoE water resource, cryosphere and climate change studies, Department of Geology, Sikkim University’ for the fellowship support for this study and the space provided for the work. Authors acknowledge ECMWF (ERA5-Land), NASA-SEDAC (population data), and USGS (Landsat-5, 7, 8, and 9 data) for open data access. We also thank open-source software and tools (QGIS, R, CDO, GrADS) for data processing, analysis, and visualization. Authors appreciated for moral support and mentorship of Dr. Rakesh Kumar Ranjan, Dr. Nishchal Wanjari, and Dr. Anil Kumar Misra. We also acknowledge Sikkim state DST for various support and help.

References

- [1] Jylhä, K., Tuomenvirta, H., Ruosteenoja, K., et al., 2010. Observed and projected future shifts of climatic zones in Europe and their use to visualize climate change information. *Weather, Climate, and Society*. 2(2), 148–167.
DOI: <https://doi.org/10.1175/2010WCAS1010.1>
- [2] Dourado, C.D.S., Oliveira, S.R.D.M., Avila, A.M.H.D., 2013. Analysis of homogeneous zones in precipitation time series in the State of Bahia. *Bragantia*. 72(2), 192–198.
DOI: <https://doi.org/10.1590/S0006-87052013000200012>
- [3] Aparecido, L.E.D.O., Rolim, G.D.S., Richetti, J., et al., 2016. Köppen, Thornthwaite and Camargo climate classifications for climatic zoning in the State of Paraná, Brazil. *Ciência e Agrotecnologia*. 40(4), 405–417.
DOI: <https://doi.org/10.1590/1413-70542016404003916>
- [4] Shaw, R., Luo, Y., Cheong, T.S., et al., 2022: Asia. *Climate Change 2022: Impacts, adaptation and vulnerability*. Cambridge University Press: Cambridge, UK and New York, NY, USA. pp. 1457–1579.
DOI: <https://doi.org/10.1017/9781009325844.012>
- [5] de Souza Rolim, G., de O. Aparecido, L.E.,

2016. Camargo, Köppen and Thornthwaite climate classification systems in defining climatological regions of the state of São Paulo, Brazil. *International Journal of Climatology*. 36(2), 636–643.
DOI: <https://doi.org/10.1002/joc.4372>
- [6] Bieniek, P.A., Bhatt, U.S., Thoman, R.L., et al., 2012. Climate divisions for Alaska based on objective methods. *Journal of Applied Meteorology and Climatology*. 51(7), 1276–1289.
DOI: <https://doi.org/10.1175/JAMC-D-11-0168.1>
- [7] Gallardo, C., Gil, V., Hagel, E., et al., 2013. Assessment of climate change in Europe from an ensemble of regional climate models by the use of Köppen-Trewartha classification. *International Journal of Climatology*. 33(9), 2157–2166.
DOI: <https://doi.org/10.1002/joc.3580>
- [8] Xin, L., 2023. Proposal of a new climate classification based on Köppen and Trewartha. *International Journal of Climatology*.
DOI: <https://doi.org/10.31223/X5CM1D>
- [9] Kottek, M., Grieser, J., Beck, C., et al., 2006. World map of the Köppen-Geiger climate classification updated. *Meteorologische Zeitschrift*. 15(3), 259–263.
DOI: <https://doi.org/10.1127/0941-2948/2006/0130>
- [10] Beck, H.E., Zimmermann, N.E., McVicar, T.R., et al., 2018. Present and future Köppen-Geiger climate classification maps at 1-km resolution. *Scientific Data*. 5, 180214.
DOI: <https://doi.org/10.1038/sdata.2018.214>
- [11] Cui, D., Liang, S., Wang, D., 2021. Observed and projected changes in global climate zones based on Köppen climate classification. *Wiley Interdisciplinary Reviews: Climate Change*. 12(3), e701.
DOI: <https://doi.org/10.1002/wcc.701>
- [12] De Castro, M., Gallardo, C., Jylha, K., et al., 2007. The use of a climate-type classification for assessing climate change effects in Europe from an ensemble of nine regional climate models. *Climatic Change*. 81(Suppl 1), 329–341.
DOI: <https://doi.org/10.1007/s10584-006-9224-1>
- [13] Kim, H.J., Wang, B., Ding, Q., et al., 2008. Changes in arid climate over North China detected by the Köppen climate classification. *Journal of the Meteorological Society of Japan*. Ser. II. 86(6), 981–990.
DOI: <https://doi.org/10.2151/jmsj.86.981>
- [14] Gabler, R.E., Peter, J.F., Trapson, M., et al., 2009. *Physical geography*. Brooks/Cole: Belmont, USA.
- [15] Alvares, C.A., Stape, J.L., Sentelhas, P.C., et al., 2013. Köppen's climate classification map for Brazil. *Meteorologische Zeitschrift*. 22(6), 711–728.
DOI: <https://doi.org/10.1127/0941-2948/2013/0507>
- [16] Bhatnagar, M., Mathur, J., Garg, V. (editors), 2019. Climate zone classification of India using new base temperature. *Proceedings of the 16th IBPSA Conference*; 2019 Sep 2–4; Rome, Italy. p. 4841–4845.
DOI: <https://doi.org/10.26868/25222708.2019.211159>
- [17] Dilinuer, T., Yao, J.Q., Chen, J., et al., 2021. Regional drying and wetting trends over Central Asia based on Köppen climate classification in 1961–2015. *Advances in Climate Change Research*. 12(3), 363–372.
DOI: <https://doi.org/10.1016/j.accre.2021.05.004>
- [18] Huang, J., Li, Y., Fu, C., et al., 2017. Dryland climate change: Recent progress and challenges. *Reviews of Geophysics*. 55(3), 719–778.
DOI: <https://doi.org/10.1002/2016RG000550>
- [19] Cheng, G., Liu, T., Wang, S., et al., 2023. Bivariate hazard assessment of combinations of dry and wet conditions between adjacent seasons in a climatic transition zone. *Atmosphere*. 14(3), 437.
DOI: <https://doi.org/10.3390/atmos14030437>
- [20] Pei, F., Zhou, Y., Xia, Y., 2021. Application of normalized difference vegetation index (NDVI) for the detection of extreme precipitation change. *Forests*. 12(5), 594.
DOI: <https://doi.org/10.3390/f12050594>
- [21] Nagai, S., Nasahara, K.N., Muraoka, H., et al., 2010. Field experiments to test the use of the

- normalized-difference vegetation index for phenology detection. *Agricultural and Forest Meteorology*. 150(2), 152–160.
DOI: <https://doi.org/10.1016/j.agrformet.2009.09.010>
- [22] Parida, B.R., Kumar, P., Chakraborty, J.S., et al., 2022. Dynamics of land use/land cover over Indian Himalayan region (IHR) using satellite data from 1985 to 2015 coupled with local perceptions. *Handbook of Himalayan ecosystems and sustainability*. CRC Press: Boca Raton. pp. 3–22.
- [23] Kumar, P., Patel, A., Rai, J., et al., 2024. Environmental challenges and concurrent trend of weather extremes over Uttarakhand Himalaya. *Theoretical and Applied Climatology*. 155(2), 1217–1246.
DOI: <https://doi.org/10.1007/s00704-023-04690-z>
- [24] Bashir, O., Bangroo, S.A., Guo, W., et al., 2022. Simulating spatiotemporal changes in land use and land cover of the north-western Himalayan Region using Markov chain analysis. *Land*. 11(12), 2276.
DOI: <https://doi.org/10.3390/land11122276>
- [25] Ghosh, S., Lata, R., Gouda, K.C., 2023. Monitoring the role of temporal land cover changes on mountain hazard susceptibility in Beas Valley, Himachal Pradesh, India. *EGU General Assembly 2023*; 2023 Apr 24–28; Vienna, Austria.
DOI: <https://doi.org/10.5194/egusphere-egu23-3919>
- [26] Kashyap, R., Pandey, A.C., Parida, B.R., 2022. Climate forcing on photosynthetic variability across various relief zones in the Himalaya. *Handbook of Himalayan ecosystems and sustainability*. CRC Press: Boca Raton. pp. 245–262.
- [27] Shafiq, M.ul, Tali, J.A., Islam, Z.ul, et al., 2022. Changing land surface temperature in response to land use changes in Kashmir valley of northwestern Himalayas. *Geocarto International*. 37(27), 18618–18637.
DOI: <https://doi.org/10.1080/10106049.2022.2142968>
- [28] Sharma, E., 1992. Integrated watershed management: A case study in Sikkim Himalaya (No. 2). G.B. Pant Institute of Himalayan Environment & Development: Uttarakhand.
- [29] Sharma, A.K., Joshi, V., Parkash, S., et al., 2009. Land Use Pattern mapping using Remote Sensing and GIS in Gangtok area, Sikkim Himalaya, India. *GIS development. net*. pp.1–2.
- [30] Sharma, N., Das, A.P., Shrestha, D.G., 2015. Landuse and landcover mapping of East District of Sikkim using IRS P6 Satellite Imagery. *Pleione*. 9(1), 193–200.
- [31] Mishra, P.K., Rai, A., Rai, S.C., 2020. Land use and land cover change detection using geospatial techniques in the Sikkim Himalaya, India. *The Egyptian Journal of Remote Sensing and Space Science*. 23(2), 133–143.
DOI: <https://doi.org/10.1016/j.ejrs.2019.02.001>
- [32] Kumar, P., Sharma, K., Malu, A., et al., 2023. Measurement report: Intra-annual variability of black/brown carbon and its interrelation with meteorological conditions over Gangtok, Sikkim. *EGUsphere*.
DOI: <https://doi.org/10.5194/egusphere-2023-702>
- [33] Uthaman, M., Singh, C., Singh, A., et al. (editors), 2023. Seismicity and active tectonics: New insights from Sikkim Himalaya. *EGU General Assembly 2023*; 2023 Apr 24–28; Vienna, Austria.
DOI: <https://doi.org/10.5194/egusphere-egu23-343>
- [34] Upadhyay, A., Rai, S.C., 2023. Climate change analysis in Rangit Basin of Sikkim Himalaya. *The Oriental Anthropologist*. 23(1), 103–130.
DOI: <https://doi.org/10.1177/0972558X221147205>
- [35] Latwal, A., Sah, P., Sharma, S., et al., 2023. Relationship between timberline elevation and climate in Sikkim Himalaya. *Ecology of Himalayan Treeline Ecotone*. Springer: Singapore.
DOI: https://doi.org/10.1007/978-981-19-4476-5_4
- [36] Shukla, A., Garg, P.K., Srivastava, S., 2018.

- Evolution of glacial and high-altitude lakes in the Sikkim, Eastern Himalaya over the past four decades (1975–2017). *Frontiers in Environmental Science*. 6, 81.
DOI: <https://doi.org/10.3389/fenvs.2018.00081>
- [37] Dash, S.K., Sharma, N., Pattnayak, K.C., et al., 2012. Temperature and precipitation changes in the north-east India and their future projections. *Global and Planetary Change*. 98–99, 31–44.
DOI: <https://doi.org/10.1016/j.gloplacha.2012.07.006>
- [38] Bhasin, M.K., Kumar, V., Sehgal, A., 1984. Impact of Human Activities on the Ecosystem and Vice-Versa with Reference to the Sikkim-Himalaya MAB (Man and Biosphere) Programme, Unesco. Mountain Research and Development, pp.267–271.
DOI: <https://doi.org/10.2307/3673146>
- [39] Chowdhury, A., De, S.K., Sharma, M.C., et al. (editors), 2022. Glacial Lakes in the Chhomo Chhu Watershed (Sikkim Himalaya, India): Inventory, Classification, Evolution, and Potential GLOFs Assessment. 10th International Conference on Geomorphology; 2022 Sep 12–16; Coimbra, Portugal.
DOI: <https://doi.org/10.5194/icg2022-19>
- [40] Basu, R., Misra, G., Sarkar, D., 2021. A remote sensing-based analysis of climate change in Sikkim supported by evidence from the field. *Journal of Mountain Science*. 18(5), 1256–1267.
DOI: <https://doi.org/10.1007/s11629-020-6534-0>
- [41] Kumar, P., Sharma, K., 2023. Snowfall shift and precipitation variability over Sikkim Himalaya attributed to elevation-dependent warming. *Journal of Atmospheric Science Research*. 6(4).
DOI: <https://doi.org/10.30564/jasr.v6i4.5854>
- [42] Singh, T., Saha, U., Prasad, V.S., et al., 2021. Assessment of newly-developed high resolution reanalyses (IMDAA, NGFS AND ERA5) against rainfall observations for indian region. *Atmospheric Research*. 259, 105679.
DOI: <https://doi.org/10.1016/j.atmosres.2021.105679>
- [43] Lal, P., Singh, G., Das, N.N., et al., 2022. Assessment of ERA5-land volumetric soil water layer product using in situ and SMAP soil moisture observations. *IEEE Geoscience and Remote Sensing Letters*. 19, 1–5.
DOI: <https://doi.org/10.1109/LGRS.2022.3223985>
- [44] Kumari, A., Raghuvanshi, A.S., Agarwal, A., 2023. Quantifying the reliability of reanalysis precipitation products across India. River, sediment and hydrological extremes: Causes, impacts and management. Disaster resilience and green growth. Springer: Singapore.
DOI: https://doi.org/10.1007/978-981-99-4811-6_6
- [45] Muñoz-Sabater, J., Dutra, E., Agustí-Panareda, A., et al., 2021. ERA5-Land: A state-of-the-art global reanalysis dataset for land applications. *Earth System Science Data*. 13(9), 4349–4383.
DOI: <https://doi.org/10.5194/essd-13-4349-2021>
- [46] Masek, J.G., Wulder, M.A., Markham, B., et al., 2020. Landsat 9: Empowering open science and applications through continuity. *Remote Sensing of Environment*. 248, 111968.
DOI: <https://doi.org/10.1016/j.rse.2020.111968>
- [47] Vermote, E., Justice, C., Claverie, M., et al., 2016. Preliminary analysis of the performance of the Landsat 8/OLI land surface reflectance product. *Remote Sensing of Environment*. 185, 46–56.
DOI: <https://doi.org/10.1016/j.rse.2016.04.008>
- [48] Aster Global Digital Elevation Model Version 2–Summary of Validation Results [Internet]. Japan-US ASTER Science Team. Available from: https://lpdaac.usgs.gov/documents/220/Summary_GDEM2_validation_report_final.pdf
- [49] Gridded Population of the World, Version 4 (GPWv4) [Internet]. Center for International Earth Science Information Network—CIESIN—Columbia University, 2016. Available from: <https://sedac.ciesin.columbia.edu/data/collection/gpw-v4>

- [50] Milovanović, B., 2017. Climate regionalization of Serbia according to Köppen climate classification. *Зборник радова Географског института “Јован Цвијић” САНУ*. 67(2), 103–114.
- [51] DeFries, R.S., Townshend, J.R.G., 1994. NDVI-derived land cover classifications at a global scale. *International Journal of Remote Sensing*. 15(17), 3567–3586.
DOI: <https://doi.org/10.1080/01431169408954345>
- [52] Gessesse, A.A., Melesse, A.M., 2019. Temporal relationships between time series CHIRPS-rainfall estimation and eMODIS-NDVI satellite images in Amhara Region, Ethiopia. *Extreme hydrology and climate variability*. Elsevier: Amsterdam. pp. 81–92.
DOI: <https://doi.org/10.1016/B978-0-12-815998-9.00008-7>
- [53] Liang, J., Ren, C., Li, Y., et al., 2023. Using enhanced gap-filling and whittaker smoothing to reconstruct high spatiotemporal resolution NDVI time series based on Landsat 8, Sentinel-2, and MODIS Imagery. *ISPRS International Journal of Geo-Information*. 12(6), 214.
DOI: <https://doi.org/10.3390/ijgi12060214>
- [54] Rao, Y., Zhu, X., Chen, J., et al., 2015. An improved method for producing high spatial-resolution NDVI time series datasets with multi-temporal MODIS NDVI data and Landsat TM/ETM+ images. *Remote Sensing*. 7(6), 7865–7891.
DOI: <https://doi.org/10.3390/rs70607865>
- [55] Ibrahim, S., Kose, M., Adamu, B., et al., 2022. Remote sensing for assessing the ecological and socio-economic impacts of forest fire severity in Kozan District, Turkey.
DOI: <https://doi.org/10.21203/rs.3.rs-2093420/v1>
- [56] Saadat, H., Adamowski, J., Bonnell, R., et al., 2011. Land use and land cover classification over a large area in Iran based on single date analysis of satellite imagery. *ISPRS Journal of Photogrammetry and Remote Sensing*. 66(5), 608–619.
DOI: <https://doi.org/10.1016/j.isprsjprs.2011.04.001>
- [57] Alturk, B., Konukcu, F., 2020. Modeling land use/land cover change and mapping morphological fragmentation of agricultural lands in Thrace Region/Turkey. *Environment, Development and Sustainability*. 22, 6379–6404.
DOI: <https://doi.org/10.1007/s10668-019-00485-3>
- [58] Potapov, P., Hansen, M.C., Pickens, A., et al., 2022. The global 2000–2020 land cover and land use change dataset derived from the Landsat archive: First results. *Frontiers in Remote Sensing*. 3, 856903.
DOI: <https://doi.org/10.3389/frsen.2022.856903>
- [59] Kim, T.K., 2015. T test as a parametric statistic. *Korean Journal of Anesthesiology*. 68(6), 540–546.
DOI: <https://doi.org/10.4097/kjae.2015.68.6.540>
- [60] Tables of P-values for T- and Chi-square Reference Distributions [Internet]. University of South Carolina. Available from: <http://math.arizona.edu/~piegorsch/571A/TR194.pdf>
- [61] Alashan, S., 2024. Non-monotonic trend analysis using Mann-Kendall with self-quantiles. *Theoretical and Applied Climatology*. 155(2), 901–910.
DOI: <https://doi.org/10.1007/s00704-023-04666-z>
- [62] Lornezhad, E., Ebrahimi, H., Rabieifar, H.R., 2023. Analysis of precipitation and drought trends by a modified Mann–Kendall method: A case study of Lorestan province, Iran. *Water Supply*. 23(4), 1557–1570.
DOI: <https://doi.org/10.2166/ws.2023.068>
- [63] Sheoran, R., Dumka, U.C. (editors), 2023. A new prewhitening approach for trend analysis in the autocorrelated time series. *EGU General Assembly 2023*; 2023 Apr 24–28; Vienna, Austria.
DOI: <https://doi.org/10.5194/egusphere-egu23-6544>
- [64] Mann, H.B., 1945. Nonparametric tests against trend. *Econometrica*. 13(3), 245–259.
DOI: <https://doi.org/10.2307/1907187>
- [65] Kendall, M.G., 1955. Further contributions to the theory of paired comparisons. *Biometrics*.

- 11(1), 43–62.
DOI: <https://doi.org/10.2307/3001479>
- [66] De, S.K., Chowdhury, A., Sharma, M.C. (editors), 2023. Inventory, classification, evolution, and potential outburst flood assessment of glacial lakes in the Chhombo Chhu Watershed (Sikkim Himalaya, India). EGU General Assembly 2023; 2023 Apr 24–28; Vienna, Austria.
DOI: <https://doi.org/10.5194/egusphere-egu23-17459>
- [67] Khawas, V., 2015. Pathways for climate resilient livelihoods: The case of a large Cardamom farming in the Dzongu Valley of the Tista River Basin, Sikkim Himalaya. Climate change in the Asia-Pacific Region. Climate change management. Springer: Cham.
DOI: https://doi.org/10.1007/978-3-319-14938-7_19
- [68] Sekhar, S., Singh, N., Singh, S.K., et al., 2023. Assessment of land utilization pattern and their relationship with surface temperature and vegetation in Sikkim, India. Advanced remote sensing for urban and landscape ecology. Advances in geographical and environmental sciences. Springer: Singapore.
DOI: https://doi.org/10.1007/978-981-99-3006-7_7
- [69] Jain, A., Rai, S.C., Sharma, E., 2000. Hydro-ecological analysis of a sacred lake watershed system in relation to land-use/cover change from Sikkim Himalaya. Catena. 40(3), 263–278.
DOI: [https://doi.org/10.1016/S0341-8162\(00\)00086-2](https://doi.org/10.1016/S0341-8162(00)00086-2)
- [70] Sah, P., Latwal, A., Sharma, S., 2023. Challenges of timberline mapping in the Himalaya: A case study of the Sikkim Himalaya. Ecology of Himalayan treeline ecotone. Springer: Singapore.
DOI: https://doi.org/10.1007/978-981-19-4476-5_6
- [71] Agrawal, A., Sharma, A.R., Tayal, S., 2014. Assessment of regional climatic changes in the Eastern Himalayan region: A study using multi-satellite remote sensing data sets. Environmental Monitoring and Assessment. 186, 6521–6536.
DOI: <https://doi.org/10.1007/s10661-014-3871-x>
- [72] Aggarwal, A., Mandal, A., 2021. Estimation of past and future mass balance of glaciers of Sikkim Himalaya using energy balance modelling approach and regional climatic projections. Journal of Climate Change. 7(3), 35–43.
DOI: <https://doi.org/10.3233/JCC210017>
- [73] Wang, R., Wang, Y., Yan, F., 2022. Vegetation growth status and topographic effects in frozen soil regions on the Qinghai-Tibet Plateau. Remote Sensing. 14(19), 4830.
DOI: <https://doi.org/10.3390/rs14194830>
- [74] Mitkari, K.V., Sofat, S., Arora, M.K., et al., 2023. Linking changes in Gangotri Glacier features derived at a large-scale with climate variability; EGU General Assembly 2023; 2023 Apr 24–28; Vienna, Austria.
DOI: <https://doi.org/10.5194/egusphere-egu23-252>
- [75] Beason, S.R., Kenyon T.R., Jost R.P., et al., 2023. Changes in glacier extents and estimated changes in glacial volume at Mount Rainier National Park, Washington, USA from 1896 to 2021. Natural Resource Report. NPS/MORA/NRR—2023/2524. National Park Service: Fort Collins, Colorado.
DOI: <https://doi.org/10.36967/2299328>
- [76] Srivastava, A., Umrao, S., Biswas, S., 2023. Exploring forest transformation by analyzing spatial-temporal attributes of vegetation using vegetation indices. International Journal of Advanced Computer Science and Applications. 14(5).
DOI: <https://doi.org/10.14569/IJACSA.2023.01405114>
- [77] Basnett, S., Kulkarni, A.V., 2019. Snow cover changes observed over Sikkim Himalaya. Environmental change in the Himalayan Region. Springer: Cham.
DOI: https://doi.org/10.1007/978-3-030-03362-0_12

- [78] Tambe, S., Arrawatia, M.L., Sharma, N., 2011. Assessing the priorities for sustainable forest management in the Sikkim Himalaya, India: A remote sensing-based approach. *Journal of the Indian Society of Remote Sensing*. 39, 555–564. DOI: <https://doi.org/10.1007/s12524-011-0110-6>
- [79] Chakma, N., Biswas, S., 2022. Long period trend analysis of precipitation and temperature of west Sikkim, India. *MAUSAM*. 73(2), 413–422. DOI: <https://doi.org/10.54302/mausam.v73i2.5484>

Supplementary materials

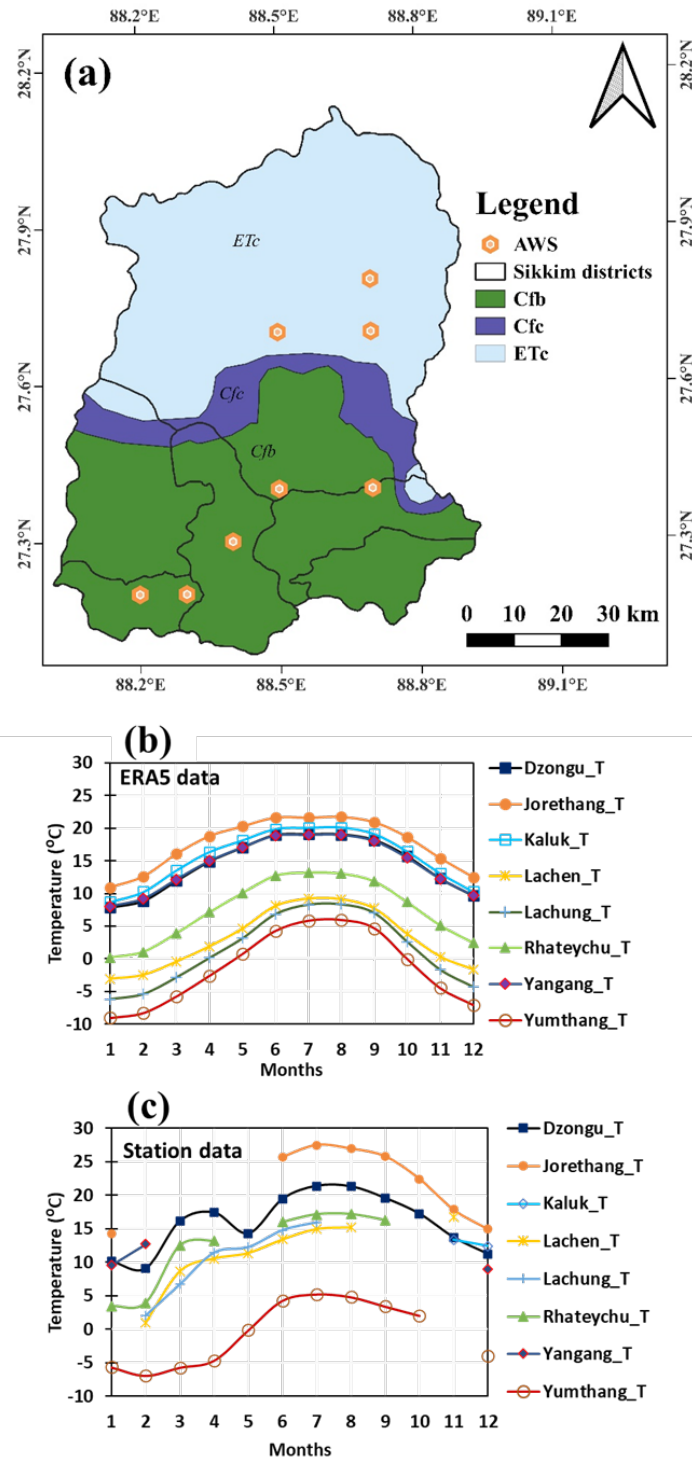


Figure S1. (a) The position of the AWS station in microclimatic zonation of ERA5-Land data. (b) ERA5-Land, and (c) AWS temperature data representation for the basic idea of the region.

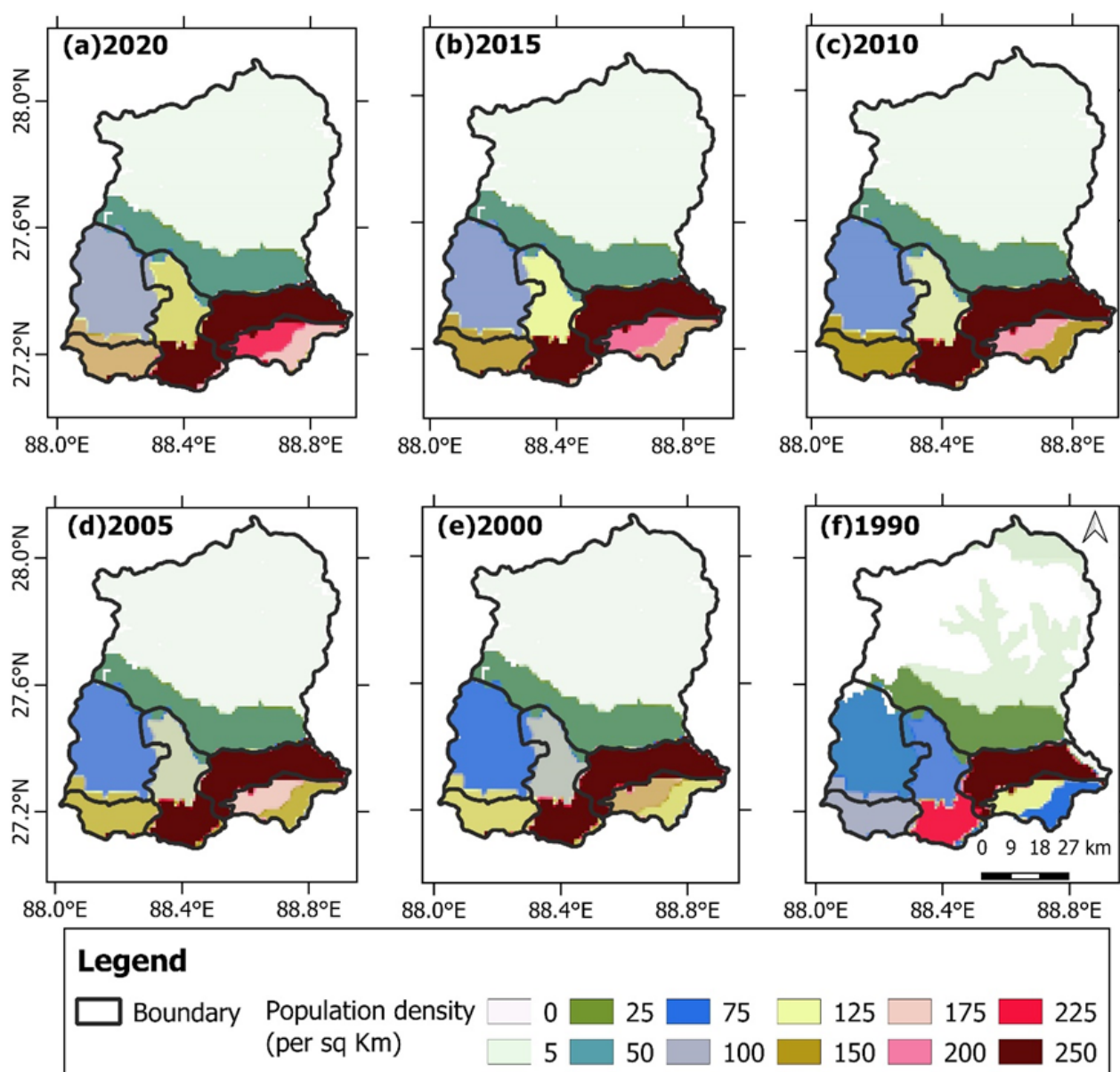


Figure S2. Population density of Sikkim for the year (1990, 2000, 2005, 2010, 2015, 2020) using SEDAC (NASA) dataset.

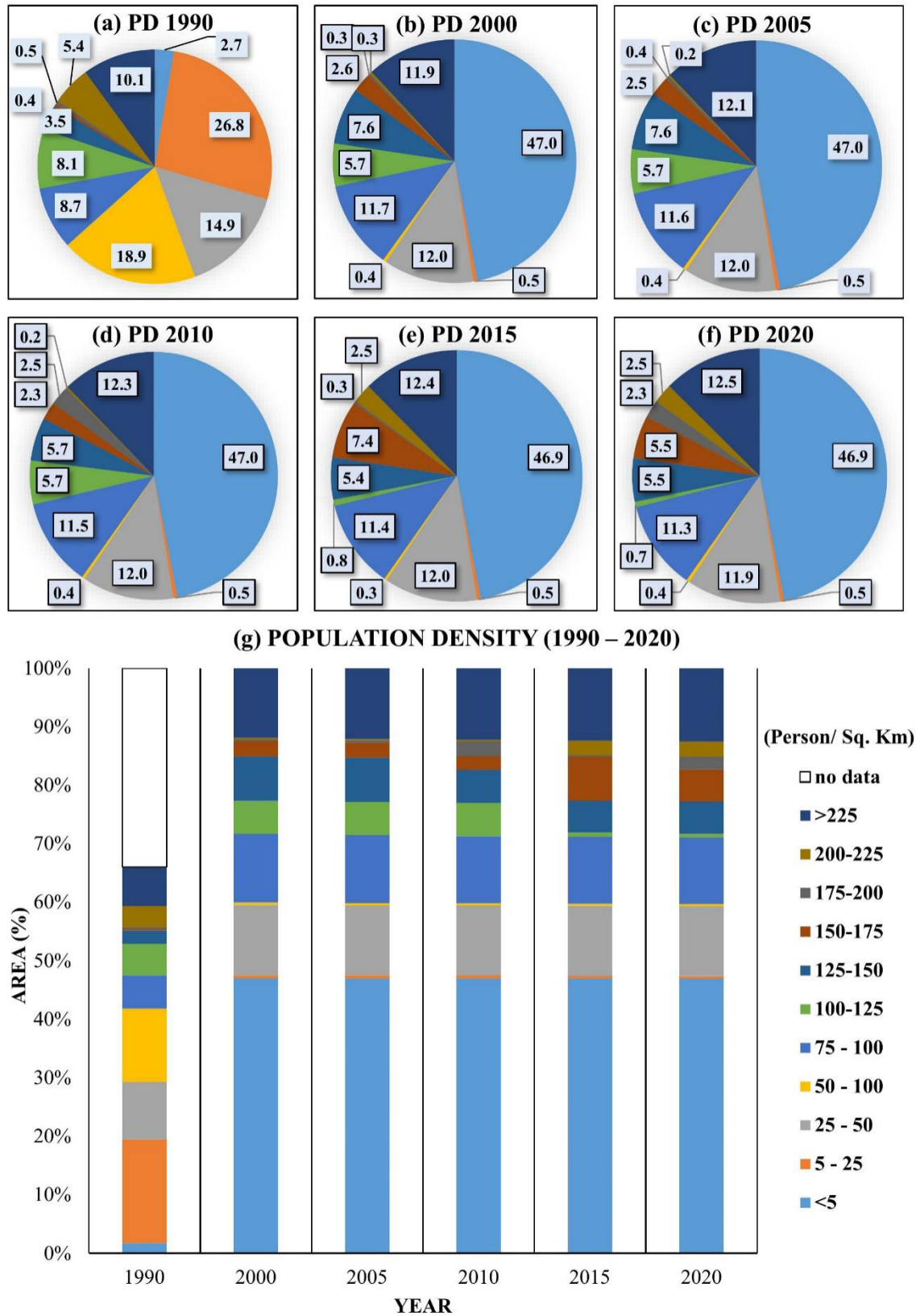


Figure S3. Population density change (percentage) of Sikkim for the study period using the SEDAC (NASA) dataset.

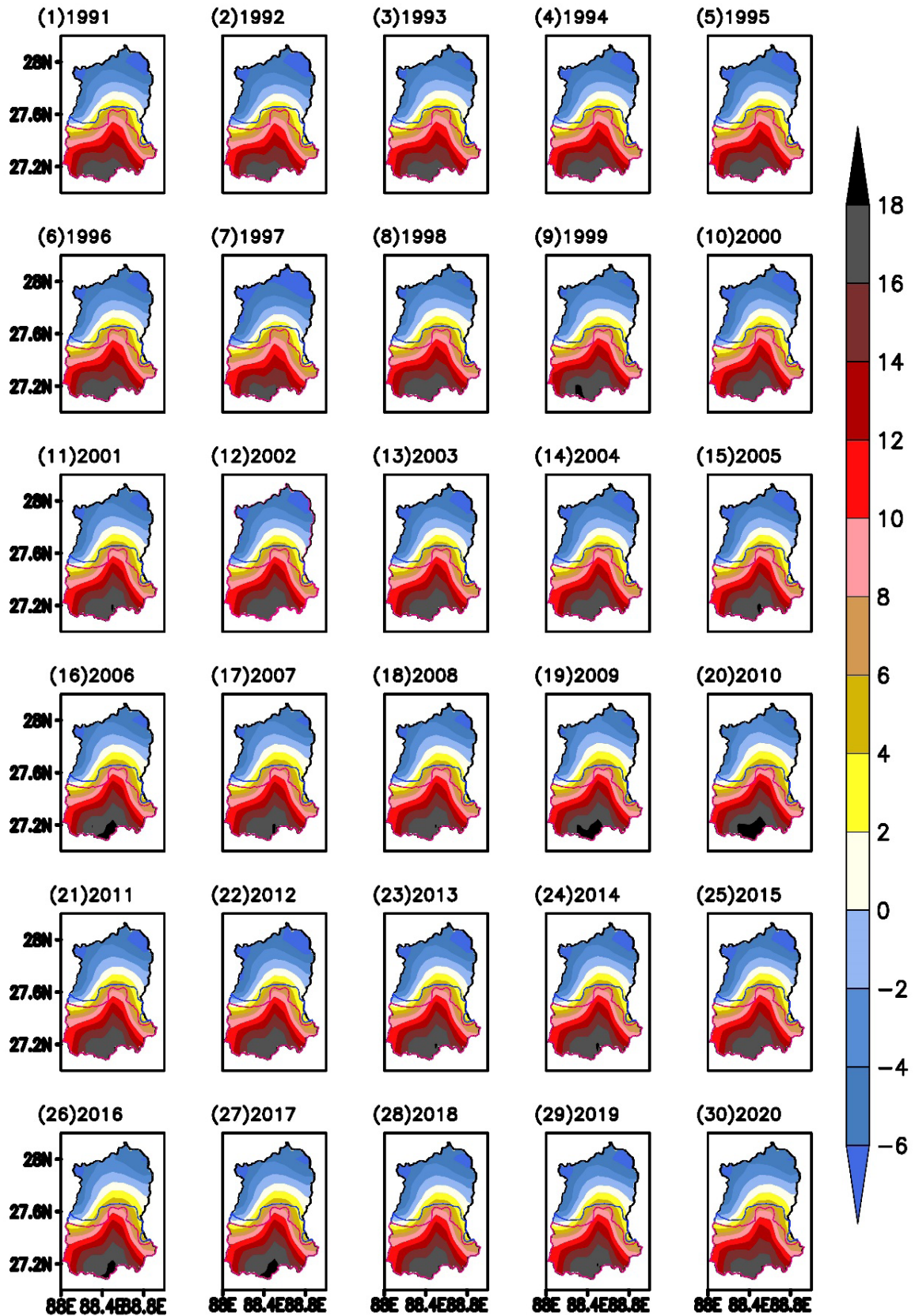


Figure S4. Spatial distribution of annual temperature for the time period of 1991 to 2020. The lines represent the climatic zonation ‘black for ETc’, ‘blue for Cfc’, and ‘magenta for Cfb’.

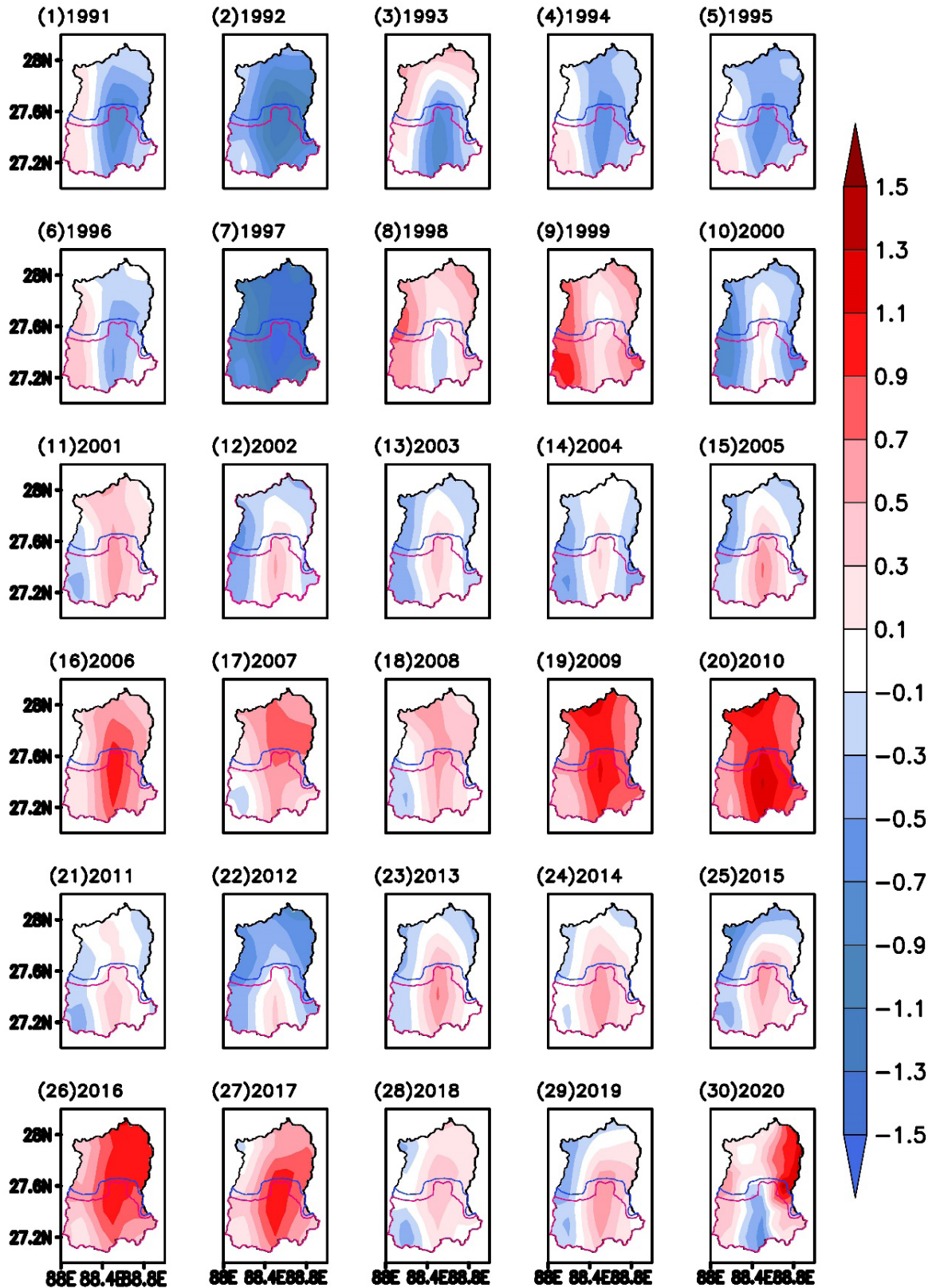


Figure S5. The spatial distribution of temperature anomaly for the periods 1991–2020 with respect to the 1980–2021 long-term average. The lines represent the climatic zonation ‘black for ETc’, ‘blue for Cfc’, and ‘magenta for Cfb’.

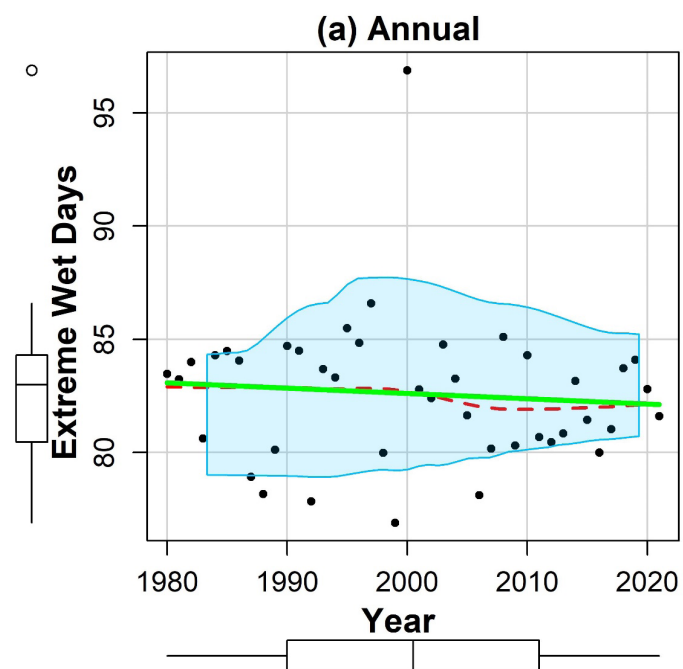


Figure S6. Man Kendall trend line with 95% significant shading of extremely wet days for 1980–2021.